
Article:
MacDonald, Chris orcid.org/0000-0002-7450-600X and Piper, Robert C (2017) Genetic dissection of early endosomal recycling highlights a TORC1-independent role for Rag GTPases. Journal of Cell Biology. pp. 3275-3290. ISSN 0021-9525

https://doi.org/10.1083/jcb.201702177

Genetic dissection of early endosomal recycling highlights a TORC1-independent role for Rag GTPases

Chris MacDonald and Robert C. Piper*

Department of Molecular Physiology and Biophysics
University of Iowa, Iowa City, IA 52246
* Correspondence: Robert-Piper@uiowa.edu

Abstract

Endocytosed cell surface membrane proteins rely on recycling pathways for their return to the plasma membrane. Although endosome-to-plasma membrane recycling is critical for many cellular processes, much of the required machinery is unknown. We discovered that yeast has a recycling route from endosomes to the cell surface that that functions efficiently following inactivation the *sec7-1* allele of Sec7, which controls transit through the Golgi. A genetic screen based an engineered synthetic reporter that exclusively follows this pathway revealed that recycling was subject to metabolic control through the Rag GTPases Gtr1 and Gtr2 which work downstream of the exchange factor Vam6. Gtr1 and Gtr2 control the recycling pathway independently of TORC1 regulation through the Gtr1 interactor Ltv1. We further show that the early-endosome recycling route and its control though the Vam6>Gtr1/Gtr2>Ltv1 pathway plays a physiological role in regulating the abundance of amino-acid transporters at the cell surface.

Introduction

Levels of cell surface membrane proteins are controlled by the balance between recycling pathways returning them to the plasma membrane and their ubiquitination and ESCRT-dependent sorting into multivesicular bodies (Maxfield and McGraw, 2004; Grant and Donaldson, 2009; Piper et al., 2014). Recycling can be regulated at the level of individual proteins through specific sorting signals, which are recognized by particular machinery (Hsu et al., 2012). In addition, overall flux through recycling pathways can be regulated globally by signal transduction and metabolic cues, as in the case for growth-factor withdrawal that causes accumulation of a broad set of nutrient transporters in intracellular compartments (Tanner and Lienhard, 1987; Corvera et al., 1986). How global regulation of recycling is orchestrated is unclear, but it is partly controlled through TORC1 signaling, which is constitutively active in some cancer cells, allowing them to sustain an elevated supply of nutrients (Edinger and Thompson, 2002; 2004). Metabolic control over the global trafficking of cell surface proteins is also observed in *Saccharomyces cerevisiae*, where a variety of membrane transporters ultimately sort to the vacuole lumen for degradation upon limitation of nitrogen, glucose, or NAD^+ (Jones et al., 2012; Lang et al., 2014; MacDonald et al., 2015; Müller et al., 2015; O'Donnell et al., 2015; Becuwe and Léon, 2014). This effect is explained in part by increased ubiquitination of the membrane protein cargoes and more efficient sorting into the multivesicular body (MVB) pathway (Babst and Odorizzi, 2013; Huber and Teis, 2016). TORC1 has been shown to influence this process in part by regulating the activity of particular Ub-ligase complexes. However, various interrelated regulatory pathways that connect TORC1 activity to ubiquitination do not adequately explain how global control of their trafficking is mediated by nutrient stress, such as nitrogen limitation (Schmidt et al., 1998; Pfannmüller et al., 2015; Merhi and André, 2012; Martín et al., 2011; MacGurn et al., 2011, Crapeau et al., 2014). One aspect that remains unclear is the extent that metabolic cues may control flux through the trafficking pathways that convey proteins back to the plasma membrane.

Recycling of membrane proteins back to the surface of mammalian cells can occur along a

variety of pathways including a rapid 'direct' pathway and slower route that passes through Rab11-positive recycling endosomes (Maxfield and McGraw, 2004), (Grant and Donaldson, 2009; Huotari and Helenius, 2011). Endocytosed recycling proteins, such as the Transferrin receptor, mainly follow these routes and very rarely transit the *trans*-Golgi network (TGN) (Snider and Rogers, 1985; Sheff et al., 1999). However, there is limited understanding of what protein machinery controls these routes and the processes that regulate flux of recycling. Recycling in yeast was first widely recognized from experiments using the styryl endocytic tracer dye, FM4-64, and the fluid phase dye Lucifer yellow, both of which are quickly secreted from yeast cells after internalization (Wiederkehr et al., 2001; 2000; Galan et al., 2001). This pathway is distinct from sorting out of late endosomes / MVBs, as FM4-64 efflux is unaltered in *vps4*Δ mutants (Wiederkehr et al., 2000), which trap MVB cargoes within exaggerated late endosomal compartments. One critical component on which this efflux pathway relies is Rcy1, an F-box protein whose function defines this process yet whose molecular function remains poorly defined. Loss of Rcy1 and other components involved in this pathway, such as the phospholipid flippase Drs2/Cdc50 complex and the Arf effector Gcs1, traps endocytosed material in early endosomes (Xu et al., 2013; Hua et al., 2002; Chen et al., 2005; Furuta et al., 2007; Robinson et al., 2006). One well-studied protein that traffics in an Rcy1-dependent route through early endosomes is the SNARE protein Snc1. Unlike the major endocytic recycling pathways in mammalian cells, return of endocytosed Snc1 to the cell surface is thought to occur mainly via transport from early endosomes back to the TGN/Golgi along a 'retrieval' pathway before transit to the cell surface (MacDonald and Piper, 2016; Feyder et al., 2015; Sebastian et al., 2012; Tanaka et al., 2011). This model is rooted in observations showing that a portion of GFP-Snc1 co-localizes with Sec7 (an Arf exchange factor that marks the TGN), and that Snc1 quickly accumulates intracellularly when proteins required for transport through the Golgi are acutely inactivated (Lewis et al., 2000; Robinson et al., 2006; Chen et al., 2005). Indeed, yeast are not currently known to have a direct surface recycling pathway(s) from early endosomes to the cell surface that bypasses a retrieval step to the TGN (MacDonald and Piper, 2016). Here we find that yeast do have such a recycling pathway from early endosomes to the plasma membrane (EE>PM). A genetic screen revealed recycling requires a signal transduction pathway operating through the Rag GTPases, which in addition to activating TORC1 (Panchaud et al., 2013b), also controls recycling through the Gtr1 effector Ltv1 in a manner that is independent of TORC1. Global control over the trafficking of cell surface proteins upon nitrogen stress is explained by the combined effects of both branches of the bifurcated Gtr1/Gtr2-Rag GTPase pathway involving the retardation of the recycling pathway and inhibition of TORC1.

Results

Cell surface recycling from early endosomes

To determine whether an EE>PM recycling route might operate in yeast, we examined the efflux of FM4-64 after a short internalization pulse, which localizes dye to numerous endosomal puncta. Flow cytometry monitoring remaining dye during showed that ~70% of the internalized FM4-64 was secreted after 10 minutes, confirming previous work demonstrating that FM4-64 efflux is rapid and extensive (Wiederkehr et al., 2000). The pool of secreted FM4-64 originated from early endosomes since high efflux rates were observed only when dye was allowed to internalize for short periods of time (**Fig 1A**). When FM4-64 was chased a further 15 minutes where it reached late endosomes and the limiting membrane of the vacuole (**Fig 1B**), only a low rate of efflux was observed. These data confirm FM4-64 can readily leave early endosomes and traffic to the plasma membrane, but that efflux from late endosomes is far slower. Similarly, cells lacking the ESCRT-associated Vps4 AAA-ATPase, which dramatically slows flux through late endosomal structures (Babst et al., 1997), had no effect on efflux of FM4-64 from early endosomal compartments, consistent with previous observations (Wiederkehr et al., 2000). To test how FM4-64 is secreted, we carried out dye efflux assays in cells harboring temperature-sensitive (*ts*) alleles of secretory pathway components: the *sec1-1* ts mutant arrests the secretory pathway at the final step of SNARE-mediated vesicle fusion to the plasma membrane, whereas the *sec7-1* ts mutant halts Arf1-dependent traffic through the TGN/Golgi apparatus (Novick et al., 1980). At

permissive-temperature (22°C) the rates of efflux in *sec1-1* and *sec7-1* cells were similar. However, at the restrictive temperature (37°C) *sec1-1* cells quickly ceased to secrete FM4-64 (**Fig. 1C**). In contrast, efflux was not slowed in *sec7-1* cells at 37°C. Previous studies have shown Snc1, a v-SNARE protein that recycles, colocalizes with the Golgi marker Sec7 and relies on Golgi function to return to the cell surface (Lewis et al., 2000; Robinson et al., 2006) thus following an itinerary from early endosomes to the TGN to join the secretory pathway back to the cell surface. In agreement, we found that when shifted to 37°C, *sec7-1* cells rapidly relocated cell-surface GFP-Snc1 to large intracellular puncta similar to the enlarged Golgi compartments that accumulate after Sec7 inactivation (Mioka et al., 2014). However, we found minimal colocalization of FM4-64 with GFP-Snc1 after inactivating Sec7, suggesting that the dye does not travel exclusively through the Golgi during its return to the cell surface (**Fig. 1D**). In contrast, Sec1 inactivation caused accumulation of both FM4-64 and GFP-Snc1 in small puncta within the same cellular regions, suggesting that Sec1 is required for the fusion of FM4-64 carrying transport intermediates with the plasma membrane. However, the extent to which GFP-Snc1 and FM4-64 occupied the same vesicular carriers or arrived at the plasma membrane in distinct carriers could not be discerned at this resolution.

We confirmed previous studies (Wiederkehr et al., 2000) that *rcy1*Δ cells are defective for FM4-64 recycling, with vacuolar delivery of the remaining dye accelerated (**Fig. 2A and 2B**). However, no effect on FM4-64 recycling (**Fig. 2B**) was found upon loss of components that mediate a retrograde retrieval route back to the TGN from endosomal compartments (e.g. retromer, Ere1, Ere2, and Snx42) (Seaman et al., 1998; Hettema, 2003; Shi et al., 2011). Together, these data indicate that a portion of internalized FM4-64 can follow a recycling route from early endosomes to the plasma membrane (EE>PM), bypassing the TGN (**Fig. 2F**). Additional phenotypes of *rcy1*Δ cells emphasized the importance of the recycling pathway. The Mup1 methionine transporter, which localizes to the cell surface in the absence of methionine, appears to travel through an Rcy1-dependent recycling route, since it is trapped within intracellular puncta in *rcy1*Δ mutants (**Fig. 2C**). Likewise, we found that growth of ***trp1*** auxotrophic cells in restricted tryptophan (Trp) conditions was dramatically compromised in *rcy1*Δ cells, indicating their inability to maintain sufficient levels of the Tat2 transporter at the cell surface (**Fig. 2D**).

An engineered reporter for the EE>PM recycling pathway

We next wanted to identify cellular machinery that was required for operating the EE>PM recycling route. This required a sensitive and well-defined reporter cargo that could be used in a genetic screen. One problem was that endogenous proteins that follow such a route might also participate in several other trafficking pathways and not be primarily constrained to the EE>PM pathway (**Fig. 2F**). Although previous studies have used Snc1 as a reporter to implicate Rcy1, alongside Drs2, Ypt31 and Ypt32, in trafficking out of early endosomes back to the plasma membrane (Galan et al., 2001; Chen et al., 2005; Liu et al., 2007; Furuta et al., 2007), it does not serve as an selective marker of a 'recycling' pathway since Snc1 can clearly follows a retrieval pathway back to the TGN/Golgi from early endosomes. Snc1 is also problematic because its distribution in the cell is highly sensitive to growth conditions (**Fig. 2E**) and is subject to increasing levels of ubiquitin (Ub)- and ESCRT-dependent sorting into the vacuole during nutrient stress (MacDonald et al., 2015; MacDonald and Piper, 2016). Mup1 might also serve as a candidate given that it is trapped within endosomes in *rcy1*Δ cells, however, our previous experiments have shown that Mup1 undergoes Ub-dependent trafficking to the vacuole when media lacks a full complement of vitamins or nitrogen, making it unreliable as a phenotypic marker in a high-throughput screen (MacDonald et al., 2015). Previous data suggest that Ste3, the **a**-factor GPCR, can cycle between endosomes and the cell surface (Davis, 1993; Roth and Davis, 1996). However, at steady state, Ste3 is largely localized in the vacuole, owing to its constitutive ubiquitination and MVB sorting (**Fig. 2E**). To engineer a better reporter protein of the EE>PM route we started with Ste3 and blocked its ability to follow the Ub- and ESCRT-dependent route to the vacuole lumen by fusing it to the catalytic domain of the UL36 deubiquitinating peptidase (DUb) and GFP for visualization by microscopy (Stringer and Piper, 2011). We reasoned that fusion of a DUb would prevent trafficking of Ste3 to the vacuole, yet still allow it to undergo internalization via its Sla1-binding NPFXD motif (Howard et al., 2002) and recycle via its natural, albeit yet uncharacterized, route back to the cell surface (**Fig. 3A**). In wild-type cells, Ste3-GFP-DUb localized almost exclusively to the plasma membrane (**Fig. 3B**), and levels of

vacuolar Pep4-processed form of GFP that is characteristic of delivery to the vacuole were minimal (**Fig. 3C**). In addition, Ste3-GFP-DUb retained its cell surface localization in cells grown to late log phase (**Fig. 3D**) when limiting nutrients cause other cell surface proteins to shunt to the vacuole and other intracellular compartments (**Fig. 2E**). In contrast, Ste3-GFP-DUb accumulated in multiple puncta in *rcy1*Δ cells where it colocalized with FM4-64 labeled early endosomes (**Fig. 3F**). The addition of the Ste3 ligand **a**-factor, which stimulates endocytosis and resulted in complete delivery of Ste3-GFP to the vacuole, had only a marginal effect on Ste3-GFP-DUb in wild-type cells. In *rcy1*Δ cells, however, **a**-factor drove the residual level of cell surface Ste3-GFP-DUb into endosomal puncta (**Fig. 3E**). Similar to FM4-64, Ste3-GFP-DUb was quickly redistributed to intracellular compartments after inactivation of Sec1, but did not appreciably accumulate in Golgi compartments after inactivation of Sec7 (**Fig. 3B**). Ste3-GFP-DUb was exclusively localized to the plasma membrane in *vps4*Δ cells (**Fig. 3G**) and not the exaggerated late endosomal compartments that accumulate ubiquitinated cargo, such as Mup1-RFP-Ub, in these mutants (Babst et al., 1997). Finally, Ste3-GFP-DUb did not accumulate in late endosomal compartments of *vps4*Δ cells when *RCY1* was additionally deleted (**Fig. 3G**). Taken together, these data support the idea that the Ste3-GFP-DUb reporter is a useful and robust proxy for assessing the function of the EE>PM recycling route, which is dependent on Rcy1 and is followed by a portion of internalized FM4-64.

Genetic dissection of the EE>PM recycling pathway

The distribution of Ste3-GFP-DUb was assessed in each of the mutants within the MAT alpha yeast haploid non-essential gene deletion collection (Winzeler, 1999). Initially, 366 mutants were identified using a liberal scoring system of any Ste3-GFP-DUb puncta. These candidates were grown under optimal conditions to reveal 89 mutants clearly defective in localizing Ste3-GFP-DUb to the cell surface. After the identity of the gene deletion was decoded from its position in the mutant array and the genotype of each mutant confirmed by PCR (**supplemental Table 1**), Ste3-GFP-DUb was localized in cells grown to mid-log phase under identical conditions and imaged for comparison (**Fig. 4A**). Mutants were also assessed for defects in FM4-64 efflux using flow cytometry (**Fig. 4B and supplemental Fig. S1b**). Finally, each candidate gene was deleted in a Trp^- auxotroph parental strain and tested for growth in limiting tryptophan (**Fig. 4C and supplemental Fig. S1c**). Collectively, the mutants identified in this screen compose the machinery controlling the EE>PM recycling pathway in yeast. Whereas some of the components have clear mechanistic links to a variety of expected functions, such as vesicle tethering, fusion, and tubule formation, others provide unanticipated links to lipid homeostasis, transcriptional programs, and metabolism, while also assigning putative functional roles for a handful of uncharacterized proteins (**supplemental Fig. S1a**). The performance of the screen was validated by its unbiased identification of *rcy1*Δ*, drs2*Δ*, cdc50*Δ, and *gcs1*Δ mutants, all of which have been previously implicated in transport from early endosomes (Galan et al., 2001; Chen et al., 2005; Liu et al., 2007; Furuta et al., 2007) (Robinson et al., 2006).. Single mutants of either *ypt31*Δ or *ypt32*Δ were defective for Ste3-GFP-DUb localization (**supplemental Fig. S2**), consistent with a specific role in recycling inferred from their physical association with Rcy1, their requirement for trafficking Snc1, and mutations within their TRAPP-II GEF complex that phenocopy the recycling defects of *rcy1*Δ mutants (Cai et al., 2007; Furuta et al., 2007; Chen et al., 2005)**.** Loss of Nhx1, the endosomal Na/H^+ exchanger, caused a profound mislocalization of Ste3-GFP-DUb to large punctate structures that are distinct from late endosomes, accumulation of intracellular Mup1-GFP, and defects in FM4-64 efflux, helping to confirm a major role for Nhx1 in endosomal trafficking, as has been proposed in yeast and mammalian cells (Bowers et al., 2000; Brett et al., 2005; Ohgaki et al., 2010; Kondapalli et al., 2015; Kojima et al., 2012). Overall, these findings validate the screen and its stringency.

Metabolic control of cell surface proteins through the EE>PM recycling pathway

We also identified Gtr1, Gtr2, and Vam6 as defective for recycling, indicating a level of regulation by nitrogen metabolism (**Fig. 5A**). Gtr1 and Gtr2, the yeast Rag GTPases, control a conserved mechanism to activate TORC1 (Powis and De Virgilio, 2016). Gtr1 and Gtr2 are localized to the limiting membrane of the vacuole via the Ego complex (Ego1 and Ego3), the yeast homolog of the Ragulator (Dubouloz et al., 2005; Binda et al., 2009). Ego-dependent localization on the vacuole allows GTP-bound

Gtr1 and GDP-bound Gtr2 (which are in their activated states) to stimulate TORC1 (Powis et al., 2015; Kira et al., 2016). Upstream of Gtr1 is Vam6, which works as an exchange factor for Gtr1 and senses leucine levels in concert with the leucyl-tRNA synthetase, Cdc60 (Bonfils et al., 2012). Cells lacking Vam6, Gtr1, or Gtr2 mislocalized Ste3-GFP-DUb to early endosomes labeled with FM4-64 (**Figs. 5B and 5C**). Like *gtr1*Δ and *gtr2*Δ mutants, loss of Vam6 also caused defects in FM4-64 efflux (**Fig. 5D**), and slow growth in limited tryptophan (**supplemental Fig. S1d**). Vam6 is known to have other cellular functions, including roles in SNARE-mediated vacuole fusion in concert with Vam2/Vps41 and the HOPS complex components Vps11, Vps16, and Vps18 (Balderhaar and Ungermann, 2013). However, loss of these other Vam6-interacting components caused no defects in recycling as measured by localization of Ste3-GFP-DUb (**Fig. 6**). Epistasis experiments confirmed that Gtr1 functions downstream of Vam6 within their pathway to control recycling since the defect in FM4-64 efflux of *vam6*Δ mutants was largely suppressed by expressing a GTP-locked mutant of Gtr1 ($Gtr1^{GTP}$) or co-expression of $Gtr1^{GTP}$ and $Gtr2^{GDP}$ (**Fig. 5D**).

The requirement of $Gtr1^{GTP}$ and $Gtr2^{GDP}$ for the recycling pathway suggested that their downstream effector TORC1 was a regulator of the pathway. However, we found that disrupting TORC1 function or disrupting the physical connection between Gtr1/Gtr2 to TORC1 had no effect on recycling. Recycling of Ste3-GFP-DUB was efficient following Rapamycin-treatment, deletion of the TORC1 subunits Tor1 or Tco89, loss of the Ego complex (yeast Ragulator) components Ego1 and Ego3, which localize Gtr1/t to the vacuole surface near TORC1 (**Fig. 6C**). In addition, Rapamycin-treatment did not inhibit FM4-64 efflux (**Fig. 6A**). Previous studies identified a number of additional proteins that function as GTPase Activating Proteins (GAPs) for Gtr1 and Gtr2 that contribute to TORC1 control (Panchaud et al., 2013a; b; Péli-Gulli et al., 2015). However, loss of Npr2, Npr3, Sea2, Sea3, Sea4 (regulators of Gtr1) or loss of Lst4 and Lst7 (regulators of Gtr2) did not effect Ste3-GFP-DUb recycling. In addition, loss of Npr2 or Sea2 had no affect on FM4-64 efflux (**Fig. 6B**). Instead, our experiments indicated an alternate downstream interactor of Gtr1, Ltv1. Previous studies demonstrated Ltv1 interacts with $Gtr1^{GTP}$ and disrupts trafficking of Gap1 (Gao and Kaiser, 2006). We found that loss of Ltv1 caused Ste3-GFP-DUb to accumulate within early endosomes (**Fig. 5C**), defects in FM4-64 efflux (**Fig. 5D**), and slow growth in media containing low levels tryptophan (**Fig. S1d**). Epistasis experiments indicated that Ltv1 functions downstream of Gtr1/Gtr2 since the defect of FM4-64 efflux of *ltv1*Δ mutants was not suppressed by expressing $Gtr1^{GTP}$ alone or in combination with $Gtr2^{GDP}$ (**Fig. 5D**). Thus, a model emerged whereby a series of multifunctional proteins collaborate within a specific metabolic pathway to execute EE>PM recycling (**Fig. 5A and 6C***).* Importantly, while Vam6, Gtr1 and Gtr2 have alternative cellular roles besides controlling EE>PM recycling, we could eliminate the possibility that these additional functions were in control of the recycling pathway (**Fig. 6C**).

We next focused on the possibility that Ltv1 also had an additional direct role in the EE>PM recycling pathway that would be distinct from its known role in ribosome biogenesis. Ltv1 is required for biogenesis of the pre40S ribosome and loss of Ltv1 causes a severe growth defect at low temperature (Seiser et al., 2006; Merwin et al., 2014; la Cruz et al., 2015). Ltv1 binds Rps3 and Rps20 to help configure the pre40S ribosome, and is then ejected prior to assembly with the 60S subunit, in a process controlled by the phosphorylation of Ltv1 by the yeast Casein Kinase, Hrr25 (Schäfer et al., 2006; Ghalei et al., 2015). However, the role of Ltv1 in recycling appeared to be independent of pre40S ribosome assembly since loss of Yar1, which works at a similar step upstream of Ltv1 (la Cruz et al., 2015), had no affect on Ste3-GFP-DUb recycling or FM4-64 efflux (**Fig. 6A and B**). To better distinguish a specific role for Ltv1 in recycling, we sought to genetically separate its potential dual roles in the cell. For this, we made a series of chimeras between Ltv1 from *Saccharomyces cerevisiae* (*Sc*) and a number of distant species including the tree mushroom, *Cylindrobasidium torrendii* (*Ct*) (**Fig. 7A**), which expressed to comparable levels (**Fig. 7B**). To preserve Ltv1 function for pre40S ribosome assembly, we made a *Ct* chimera (*Ct*-$Ltv1^{Sc\_Rps3/20}$) containing the known Rsp3 and Rps20-interacting regions from *Sc* while also changing the Hrr25 phosphorylation sites to glutamate residues, to circumvent the need for Hrr25-dependent phosphorylation (Ghalei et al., 2015). We expressed these chimeras from a low-copy plasmid in *ltv1*Δ cells and compared these cells to either wild-type cells or *ltv1*Δ cells expressing the Sc-$Ltv1^{S>E}$ allele comprised of Sc *LTV1* also carrying the glutamate residue substitutions. Whereas Sc-$Ltv1^{S>E}$ fully restored FM4-64 efflux and normal growth to *ltv1*Δ mutants, *Ct*-$Ltv1^{Sc\_Rps3/20}$ was defective for FM4-64 efflux but still restored growth *ltv1*Δ mutants (**Fig. 7C and D**). These data show that the role of Ltv1 in

recycling can be clearly dissected from its general role in ribosome assembly and growth. We also found alleles that could partially operate in an opposite manner. Here we found that an *Sc* chimera (*Sc*-Ltv1$^{Ct_Rps3/20}$) in which the Rsp3 and Rps20 binding regions were replaced with the corresponding regions from *Ct* had a severe growth defect at low temperature yet could partly suppress the FM4-64 recycling defect of *ltv1*Δ mutants (**Fig. 7C and D**).

Localization experiments buttress the model whereby Gtr1/Gtr2 and Ltv1 work directly on the recycling pathway. In wild-type cells (**Fig. 7E**), mCherry tagged Gtr1 and Gtr2, as well as their activated mutant forms (Gtr1^{GTP} and Gtr2^{GDP}) were localized diffusely in the cytosol as well as on the limiting membrane of the vacuole, consistent with previous observations (Powis et al., 2015; Kira et al., 2016). We found that GFP-tagged Ltv1 was mostly localized to the cytosol with moderate accumulation in the nucleus, consistent with previous studies (Seiser et al., 2006; Merwin et al., 2014). If Gtr1/Gtr2 and Ltv1 transiently associate with endosomes, we reasoned that they might be captured there in mutants that accumulate intermediates along this pathway. Therefore, we performed localization experiment in *nhx1*Δ mutants that accumulate large early endosomal structures that capture cargoes such as Ste3-GFP-Ub, FM4-64, and Mup1-GFP (**supplemental Fig. S2**). Loss of Nhx1 caused a distinct relocalization pattern for Gtr1, Gtr2 and Ltv1 in which Ltv1-GFP localizes to Gtr1 and Gtr2 containing puncta (**Fig. 7F**). Moreover, Gtr1 and Gtr2 also colocalized with intracellular Ste3-GFP-DUb. Co-localization of Gtr1-RFP with Ste3-GFP-DUb to intracellular puncta in *nhx1*Δ cells was compromised upon further loss of Ltv1 suggesting that Ltv1 may have a role in recruiting Gtr1 to endosomal structures. Other recycling pathway mutants, such as *drs2*Δ (**Fig. 7G**) did not accumulate Gtr1 in endosomal structures suggesting the intermediates accumulated in *nhx1*Δ mutants are qualitatively different that those in *drs2*Δ mutants or that Drs2 is part of the protein recruitment machinery for Gtr1 and its associated cohort.

We next assessed how the Vam6>Gtr1/Gtr2>Ltv1 pathway might control the recycling pathway in a physiological context. Vam6 is part of the mechanism that senses leucine, conveying that signal to Gtr1 to regulate TORC1 (Binda et al., 2009; Valbuena et al., 2012). We found that leucine starvation also blocked recycling, observed by Ste3-GFP-DUb mislocalization (**Fig. 8A**) and retardation of FM4-64 efflux (**Fig. 8B**). The defect in FM4-64 efflux could be suppressed by expressing the activated Gtr1^{GTP} protein (**Fig. 8B**), supporting the model that leucine signals through the Vam6>Gtr1/Gtr2>Ltv1 pathway to control recycling. We next determined how regulation of the recycling pathway could play a role in the overall trafficking of cell surface proteins. Mup1-GFP recycling is defective when the Vam6>Gtr1/Gtr2 pathway is disrupted (**Fig. 8C**) and previous studies have shown that nutrient depletion, specifically starvation for leucine, can cause proteins such as Mup1 to traffic to the vacuole (Jones et al., 2012). This effect partly relies on Ub- and ESCRT-mediated trafficking through the MVB pathway, which is responsible for packaging membrane proteins into endosomal lumenal vesicles. Whereas TORC1 inhibition causes global upregulation of Rsp5 activity (Iesmantavicius et al., 2014) and TORC1 activity controls trafficking of nutrient transporters, opposing modes of TORC1 control over individual transporters have been described. Some stimuli that activate TORC1 cause amino-acid transporters such as Can1, Mup1, and Gap1 to traffic to the vacuole through activation of particular arrestin-related substrate-adaptors of the Rsp5 ligase (Schmidt et al., 1998; Pfannmüller et al., 2015; Merhi and André, 2012; Martín et al., 2011; MacGurn et al., 2011; Crapeau et al., 2014). This mechanism does not explain how leucine-starvation, which would inactivate TORC1, results in rapid withdrawal of transporters from the cell surface. An alternative explanation is that the effect of leucine starvation reflects a compound phenotype of both TORC1 inactivation and regulation of the recycling pathway via Ltv1, since both would be controlled by the Leucine>Cdc60>Vam6>Gtr1 signaling pathway. **Figure 8D** supports this model in that acute inhibition of TORC1 with Rapamycin had no effect on the cell surface localization of Mup1. Yet in *ltv1*Δ mutants, where the other branch of the Gtr1 pathway is blocked, Rapamycin had a dramatic effect on sorting Mup1-GFP to the vacuole that mimicked the full effect of leucine-starvation.

Discussion

Discovery of an EE>PM pathway in yeast and identification of its molecular machinery using a dedicated synthetic reporter helps clarify functions for a number of proteins that have clear mammalian homologs (**supplemental Table 2**). These studies also reveal a mechanistic framework for how EE>PM

recycling can be regulated by signal transduction pathways that integrate the overall metabolic activity of the cell. Both Snc1 and Ste3-GFP-DUb are internalized from the cell surface and travel out of early endosomes before reaching late endosomes. Both of these cargoes are trapped within early endosomes in cells lacking some of the known protein machinery required for transport out of early endosomes including Rcy1, Drs2, Cdc50, and the Arf-GAP Gcs1 (Wiederkehr et al., 2000; Hua et al., 2002; Robinson et al., 2006; Chen et al., 2006). We find that the Ste3-GFP-DUb reporter stayed confined to an early endosome/PM itinerary in that it did not travel through late endosomes that accumulate class E/ESCRT Vps mutants and it did not undergo ubiquitin-dependent sorting into multivesicular bodies. Ste3-GFP-DUb also did not accumulate in Golgi structures in *sec7*-ts cells at the non-permissive temperature under conditions where GFP-Snc1 did. This suggests that while flux of internalized GFP-Snc1 through the *sec7-1* sensitive step through the Golgi is substantial, that of Ste3-GFP-DUb is much less; together illustrating that the route Snc1 takes from endosomes is demonstrably distinct from that of Ste3-GFP-DUb. Importantly, Ste3-GFP-DUb did accumulate intracellularly upon acute loss of Sec1 function (via a *sec1*-ts allele), showing that the bulk of Ste3-GFP-DUb is internalized and recycled within the timeframe of our experiments. These data imply that both Golgi-derived and endosome-derived transport intermediates use a Sec1-sensitive step for fusion with the plasma membrane. Such a model is consistent with data from animal cells where a cohort of highly homologous SNAREs and associated proteins function in both secretory and endosome derived transport intermediates to mediate fusion with the plasma membrane (Hong and Lev, 2014; Huynh et al., 2007). Here, such a model obliges that Snc1/2 would populate both intermediates. Retrieval of Snc1 from early endosomes back to the TGN/Golgi has been clearly established (Lewis et al., 2000; Robinson et al., 2006; Chen et al., 2005; Galan et al., 2001). Whereas these data clearly show that a major flux of endosomal Snc1 back to the plasma membrane can travel through TGN/Golgi compartments, they do not exclude the possibility that Snc1 also travels through other pathways, such as the EE>PM pathway proposed here, which bypasses the TGN/Golgi.

In contrast to Snc1, the Ste3-GFP-DUb reporter behaved more similarly to FM4-64, as it did not readily accumulate in Golgi-like compartments upon inactivation of Sec7 under our experimental conditions. We note that previous experiments have shown localization of FM4-64 to Sec7 positive compartments, concluding FM4-64 traveled back to the Golgi apparatus during its return to the cell surface (Lewis et al., 2000; Bhave et al., 2014). In our experiments, inactivation of Sec7 accumulated Snc1 in compartments markedly distinct from endosomal populations of FM4-64, and dye efflux remained efficient when transit through the Golgi was blocked. One of the difficulties in following FM4-64 is that it travels along multiple pathways and the basis of its trafficking (as a styrl dye, it binds to a complex of lipids that remain unknown) is unclear. After internalization, some FM4-64 travels to the limiting membrane of the vacuole, and a different portion is effluxed out of the cell. Even the mutants with defective in FM4-64 recycling exhibit a sizable rate of residual FM4-64 efflux (**Fig. 4 and S1**). Furthermore, we found that some of these defects are additive, whereby FM4-64 efflux is far worse in an *ltv1*Δ *nhx1*Δ double mutant than it is in either single mutant (**supplemental Fig. S3g**). This could either indicate that loss of each gene results in a partial block of the same pathway, or that multiple pathways for FM4-64 efflux exist. It may be that compromise of one pathway would shunt FM4-64 through a different one, including a route via the Golgi apparatus. As Ste-GFP-DUb and the bulk of FM4-64 appeared to follow a recycling route that bypasses the Golgi, and most of the mutants defective for Ste3-GFP-DUb localization had defects in FM4-64 efflux, we conclude both cargoes mainly report on the direct EE>PM pathway.

For those proteins with less defined roles in the endocytic pathway, discovering a role for them in EE>PM recycling potentially clarifies their primary function. One such protein is Nhx1, an Na+/H+ exchanger localized to early endosomal compartments (Kojima et al., 2012). Loss of Nhx1 in yeast causes changes in late endosome function reminiscent of ESCRT mutants, which have defects in MVB biogenesis and accumulate cargo proteins within enlarged late endosomes (Bowers et al., 2000). We find that *nhx1*Δ mutants accumulate Ste3-GFP-DUb in endosomal compartments that are distinct from the late endosomal structures that accumulate in ESCRT-deficient cells (**supplemental Fig. S3**), consistent with data from both yeast and animal cells indicating a direct role for Nhx1 in trafficking through early endosomes. Also defective in recycling were mutants lacking Ist1, a protein structurally related to ESCRT-III subunits and that binds to the Vps4 AAA-ATPase. Mutant *ist1*Δ cells are defective in

Ste3-GFP-DUb and Mup1 localization, FM4-63 efflux and growth in low tryptophan (**supplemental Fig. S1 and S3**). Ist1 is not strictly required for ESCRT-dependent sorting into the MVB pathway (Dimaano et al., 2008; Jones et al., 2012; Rue et al., 2008). Recent experiments implicate Ist1 in scission of tubules emanating from early endosomes (Allison et al., 2013) and cryo-EM studies indicate that Ist1 can bend membranes in a manner that is topologically distinct from scission of lumenal vesicles mediated by ESCRT-III (McCullough et al., 2015). A distinct role for Ist1 in promoting recycling also fits with previous observations that show delivery of cargo into the MVB pathway is accelerated in the absence of Ist1, which would otherwise rescue cell surface proteins from degradation. We further found that recycling is supported by mutants of Ist1 that lack their **M**IT-**i**nteraction **m**otif (MIM), which is required for its functional interaction with Vps4 (Shestakova et al., 2010), underscoring a role for Ist1 that is distinct from ESCRT-III and Vps4 related functions on late endosomes (**supplemental Fig. S2**). It has been reported that Ist1 is a heavily ubiquitinated and unstable protein whose levels may be affected by various stresses and metabolic conditions (Jones et al., 2012) raising the possibility that the recycling defects of some of the mutants we uncovered were due to decreased levels of Ist1. However, Ist1 levels appear unchanged in a wide variety of recycling mutants suggesting that their recycling defects are not due to simple loss of Ist1 function (**supplemental Fig. S2**).

Nutritional control over the recycling pathway may serve as a way to synchronize surface protein activity (e.g. amino acid transport) with metabolic activity of the cell. As shown previously, starvation for leucine shunts a wide variety of cell surface proteins to the vacuole (Jones et al., 2012) . We propose that leucine starvation regulates two coordinated, yet distinct, pathways through the Rag GTPases, Gtr1 and Gtr2. Firstly, surface protein retention in endosomes is achieved by inhibition of the Gtr1/Gtr2>Ltv1 recycling pathway. Secondly, the sorting of endosomally-localized cargo into the MVB pathway is elevated through inhibition of TORC1. It is not yet clear what molecular function Ltv1 provides to promote recycling, nor how it localizes Gtr1/Gtr2 to endosomes. Ltv1 functions in the assembly or ribosomes and is required for robust growth at lower temperature, yet this alternative function could be genetically separated from its role in the recycling pathway The effect of Gtr1 and Gtr2 specifically on the recycling pathway is independent of TORC1, since their localization and communication with TORC1 on the vacuole is dependent on the Ego complex, loss of which has no effect on recycling. In addition, acute inhibition of TORC1 with Rapamycin or compromise of TORC1 activity by knocking out the nonessential subunits *TOR1* and *TCO89* also had no effect. TORC1 does have an effect on the trafficking of cell surface proteins, which is ultimately determined by increased flux through the MVB pathway by increased ubiquitination of cargo. These combined effects speak to complex layers of regulation for nutrient transporters, which we can mimic by the combined inhibition of the recycling pathway (via *ltv1*Δ mutation) and acute inhibition of TORC1 with a short treatment with Rapamycin (**Fig. 8D**). This model complements previous work implicating the Rag GTPases and EGO complex in trafficking of the amino-acid transporter Gap1 (Gao and Kaiser, 2006). Those studies showed loss of Gtr1, the Ego complex, or Ltv1 diminishes both total cellular levels and cell surface levels of Gap1. The effect of the Ego complex mutants would explained by compromise of TORC1 function, and is consistent with the effects of longer term Rapamycin-treatment on the ubiquitination and MVB sorting of Gap1, as well as additional transporters shown in other studies (Crapeau et al., 2014). In contrast, loss of another Gtr1 downstream target Ltv1 inhibits return of endocytosed transporters along the EE>PM pathway, sequestering them from the cell surface and increasing their exposure the ubiquitination and MVB trafficking machinery. Such a model emphasizes the intricacies in following endogenous cell surface proteins such as Gap1, that are subject to a variety of trafficking steps at the cell surface, TGN, early endosomes, and MVBs, where many are controlled by ubiquitination (Babst and Odorizzi, 2013; Huber and Teis, 2016). By following Ste3-GFP-DUb and FM4-64, the effects on cargo ubiquitination and specific sorting sequences can be uncoupled, allowing the EE>PM recycling pathway to be revealed.

Acknowledgements
We thank members of the laboratory for constructs, advice and helpful discussions. We thank Stanley Winistorfer for help with Ltv1 chimeras, Justin Fishbaugh and the CCOM Flow cytometry facility for help with FM4-64 efflux assays. We are grateful to Claudio De Virgilio, Deborah Lycan, Dave Katzmann and Jeremy Thorner for sharing reagents. The authors would like to thank Phyllis Hanson and Markus Babst

for insightful conversations regarding Ist1 function. This work was supported by AHA post-doctoral fellowship award 13POST 14710042 to CM and NIH RO1GM058202 to RCP.

Author contributions
CM and RCP conceived and designed experiments. CM performed experiments. CM and RCP wrote the manuscript.

Competing financial interests
The authors declare no competing financial interests.

References

Allison, R., J.H. Lumb, C. Fassier, J.W. Connell, D. Ten Martin, M.N.J. Seaman, J. Hazan, and E. Reid. 2013. An ESCRT-spastin interaction promotes fission of recycling tubules from the endosome. *J. Cell Biol.* 202:527–543. doi:10.1083/jcb.201211045.

Babst, M., and G. Odorizzi. 2013. The balance of protein expression and degradation: an ESCRTs point of view. *Current Opinion in Cell Biology*. 25:489–494. doi:10.1016/j.ceb.2013.05.003.

Babst, M., T.K. Sato, L.M. Banta, and S.D. Emr. 1997. Endosomal transport function in yeast requires a novel AAA-type ATPase, Vps4p. *EMBO J.* 16:1820–1831. doi:10.1093/emboj/16.8.1820.

Balderhaar, H.J.K., and C. Ungermann. 2013. CORVET and HOPS tethering complexes - coordinators of endosome and lysosome fusion. *J. Cell. Sci.* 126:1307–1316. doi:10.1242/jcs.107805.

Becuwe, M., and S. Léon. 2014. Integrated control of transporter endocytosis and recycling by the arrestin-related protein Rod1 and the ubiquitin ligase Rsp5. *eLife*. 3. doi:10.7554/eLife.03307.

Bhave, M., E. Papanikou, P. Iyer, K. Pandya, B.K. Jain, A. Ganguly, C. Sharma, K. Pawar, J. Austin, K.J. Day, O.W. Rossanese, B.S. Glick, and D. Bhattacharyya. 2014. Golgi enlargement in Arf-depleted yeast cells is due to altered dynamics of cisternal maturation. *J. Cell. Sci.* 127:250–257. doi:10.1242/jcs.140996.

Binda, M., M.-P. Péli-Gulli, G. Bonfils, N. Panchaud, J. Urban, T.W. Sturgill, R. Loewith, and C. De Virgilio. 2009. The Vam6 GEF controls TORC1 by activating the EGO complex. *Mol. Cell*. 35:563–573. doi:10.1016/j.molcel.2009.06.033.

Bonfils, G., M. Jaquenoud, S. Bontron, C. Ostrowicz, C. Ungermann, and C. De Virgilio. 2012. Leucyl-tRNA synthetase controls TORC1 via the EGO complex. *Mol. Cell*. 46:105–110. doi:10.1016/j.molcel.2012.02.009.

Bowers, K., B.P. Levi, F.I. Patel, and T.H. Stevens. 2000. The Sodium/Proton Exchanger Nhx1p Is Required for Endosomal Protein Trafficking in the Yeast Saccharomyces cerevisiae. *Mol. Biol. Cell*. 11:4277–4294. doi:10.1091/mbc.11.12.4277.

Brett, C.L., D.N. Tukaye, S. Mukherjee, and R. Rao. 2005. The Yeast Endosomal Na+(K+)/H+ Exchanger Nhx1 Regulates Cellular pH to Control Vesicle Trafficking. *Mol. Biol. Cell*. 16:1396–1405. doi:10.1091/mbc.E04-11-0999.

Cai, H., K. Reinisch, and S. Ferro-Novick. 2007. Coats, Tethers, Rabs, and SNAREs Work Together to Mediate the Intracellular Destination of a Transport Vesicle. *Developmental Cell*. 12:671–682. doi:10.1016/j.devcel.2007.04.005.

Chen, S., J. Wang, B.-P. Muthusamy, K. Liu, S. Zare, R.J. Andersen, and T.R. Graham. 2006. Roles for the Drs2p-Cdc50p complex in protein transport and phosphatidylserine asymmetry of the yeast plasma membrane. *Traffic*. 7:1503–1517. doi:10.1111/j.1600-0854.2006.00485.x.

Chen, S.H., S. Chen, A.A. Tokarev, F. Liu, G. Jedd, and N. Segev. 2005. Ypt31/32 GTPases and their novel F-box effector protein Rcy1 regulate protein recycling. *Mol. Biol. Cell*. 16:178–192. doi:10.1091/mbc.E04-03-0258.

Corvera, S., R.J. Davis, P.J. Roach, A. DePaoli-Roach, and M.P. Czech. 1986. Mechanism of receptor kinase action on membrane protein recycling. *Ann. N. Y. Acad. Sci.* 488:419–429.

Crapeau, M., A. Merhi, and B. André. 2014. Stress conditions promote yeast Gap1 permease ubiquitylation and down-regulation via the arrestin-like Bul and Aly proteins. *J. Biol. Chem.* 289:22103–22116. doi:10.1074/jbc.M114.582320.

Davis, N.G. 1993. Cis- and trans-acting functions required for endocytosis of the yeast pheromone receptors. *J. Cell Biol.* 122:53–65. doi:10.1083/jcb.122.1.53.

Dimaano, C., C.B. Jones, A. Hanono, M. Curtiss, and M. Babst. 2008. Ist1 regulates Vps4 localization and assembly. *Mol. Biol. Cell*. 19:465–474. doi:10.1091/mbc.E07-08-0747.

Dubouloz, F., O. Deloche, V. Wanke, E. Cameroni, and C. De Virgilio. 2005. The TOR and EGO protein complexes orchestrate microautophagy in yeast. *Mol. Cell*. 19:15–26. doi:10.1016/j.molcel.2005.05.020.

Edinger, A.L., and C.B. Thompson. 2002. Akt maintains cell size and survival by increasing mTOR-dependent nutrient uptake. *Mol. Biol. Cell*. 13:2276–2288. doi:10.1091/mbc.01-12-0584.

Edinger, A.L., and C.B. Thompson. 2004. An activated mTOR mutant supports growth factor-independent, nutrient-dependent cell survival. *Oncogene*. 23:5654–5663. doi:10.1038/sj.onc.1207738.

Feyder, S., J.-O. De Craene, S. Bär, D.L. Bertazzi, and S. Friant. 2015. Membrane trafficking in the yeast Saccharomyces cerevisiae model. *Int J Mol Sci*. 16:1509–1525. doi:10.3390/ijms16011509.

Furuta, N., K. Fujimura-Kamada, K. Saito, T. Yamamoto, and K. Tanaka. 2007. Endocytic recycling in yeast is regulated by putative phospholipid translocases and the Ypt31p/32p-Rcy1p pathway. *Mol. Biol. Cell*. 18:295–312. doi:10.1091/mbc.E06-05-0461.

Galan, J.-M., A. Wiederkehr, J.H. Seol, R. Haguenauer-Tsapis, R.J. Deshaies, H. Riezman, and M. Peter. 2001. Skp1p and the F-Box Protein Rcy1p Form a Non-SCF Complex Involved in Recycling of the SNARE Snc1p in Yeast. *Mol. Cell. Biol.* 21:3105–3117. doi:10.1128/MCB.21.9.3105-3117.2001.

Gao, M., and C.A. Kaiser. 2006. A conserved GTPase-containing complex is required for intracellular sorting of the general amino-acid permease in yeast. *Nat. Cell Biol.* 8:657–667. doi:10.1038/ncb1419.

Ghalei, H., F.X. Schaub, J.R. Doherty, Y. Noguchi, W.R. Roush, J.L. Cleveland, M.E. Stroupe, and K. Karbstein. 2015. Hrr25/CK1δ-directed release of Ltv1 from pre-40S ribosomes is necessary for ribosome assembly and cell growth. *J. Cell Biol.* 208:745–759. doi:10.1083/jcb.201409056.

Gietz, R.D., and R.H. Schiestl. 2007. Microtiter plate transformation using the LiAc/SS carrier DNA/PEG method. *Nat Protoc*. 2:5–8. doi:10.1038/nprot.2007.16.

Grant, B.D., and J.G. Donaldson. 2009. Pathways and mechanisms of endocytic recycling. *Nat. Rev. Mol. Cell Biol.* 10:597–608. doi:10.1038/nrm2755.

Hettema, E.H. 2003. Retromer and the sorting nexins Snx4/41/42 mediate distinct retrieval pathways from yeast endosomes. *EMBO J.* 22:548–557. doi:10.1093/emboj/cdg062.

Hong, W., and S. Lev. 2014. Tethering the assembly of SNARE complexes. *Trends in Cell Biology*. 24:35–43. doi:10.1016/j.tcb.2013.09.006.

Howard, J.P., J.L. Hutton, J.M. Olson, and G.S. Payne. 2002. Sla1p serves as the targeting signal recognition factor for NPFX (1,2)D-mediated endocytosis. *J. Cell Biol.* 157:315–326. doi:10.1083/jcb.200110027.

Hsu, V.W., M. Bai, and J. Li. 2012. Getting active: protein sorting in endocytic recycling. *Nat. Rev. Mol. Cell Biol.* 13:323–328. doi:10.1038/nrm3332.

Hua, Z., P. Fatheddin, and T.R. Graham. 2002. An essential subfamily of Drs2p-related P-type ATPases is required for protein trafficking between Golgi complex and endosomal/vacuolar system. *Mol. Biol. Cell*. 13:3162–3177. doi:10.1091/mbc.E02-03-0172.

Huber, L.A., and D. Teis. 2016. Lysosomal signaling in control of degradation pathways. *Current Opinion in Cell Biology*. 39:8–14. doi:10.1016/j.ceb.2016.01.006.

Huotari, J., and A. Helenius. 2011. Endosome maturation. *EMBO J.* 30:3481–3500. doi:10.1038/emboj.2011.286.

Huynh, K.K., J.G. Kay, J.L. Stow, and S. Grinstein. 2007. Fusion, fission, and secretion during phagocytosis. *Physiology (Bethesda)*. 22:366–372. doi:10.1152/physiol.00028.2007.

Iesmantavicius, V., B.T. Weinert, and C. Choudhary. 2014. Convergence of ubiquitylation and phosphorylation signaling in rapamycin-treated yeast cells. 13:1979–1992. doi:10.1074/mcp.O113.035683.

Jones, C.B., E.M. Ott, J.M. Keener, M. Curtiss, V. Sandrin, and M. Babst. 2012. Regulation of Membrane Protein Degradation by Starvation-Response Pathways. *Traffic*. 13:468–482. doi:10.1111/j.1600-0854.2011.01314.x.

Kira, S., Y. Kumano, H. Ukai, E. Takeda, A. Matsuura, and T. Noda. 2016. Dynamic relocation of the TORC1-Gtr1/2-Ego1/2/3 complex is regulated by Gtr1 and Gtr2. *Mol. Biol. Cell*. 27:382–396. doi:10.1091/mbc.E15-07-0470.

Kojima, A., J.Y. Toshima, C. Kanno, C. Kawata, and J. Toshima. 2012. Localization and functional requirement of yeast Na+/H+ exchanger, Nhx1p, in the endocytic and protein recycling pathway. *Biochim. Biophys. Acta*. 1823:534–543. doi:10.1016/j.bbamcr.2011.12.004.

Kondapalli, K.C., J.P. Llongueras, V. Capilla-González, H. Prasad, A. Hack, C. Smith, H. Guerrero-Cázares, A. Quiñones-Hinojosa, and R. Rao. 2015. A leak pathway for luminal protons in endosomes drives oncogenic signalling in glioblastoma. *Nat Comms*. 6:6289. doi:10.1038/ncomms7289.

Kuchler, K., R.E. Sterne, and J. Thorner. 1989. Saccharomyces cerevisiae STE6 gene product: a novel pathway for protein export in eukaryotic cells. *EMBO J.* 8:3973–3984.

la Cruz, de, J., K. Karbstein, and J.L. Woolford. 2015. Functions of ribosomal proteins in assembly of eukaryotic ribosomes in vivo. *Annu. Rev. Biochem.* 84:93–129. doi:10.1146/annurev-biochem-060614-033917.

Lang, M.J., J.Y. Martinez-Marquez, D.C. Prosser, L.R. Ganser, D. Buelto, B. Wendland, and M.C. Duncan. 2014. Glucose starvation inhibits autophagy via vacuolar hydrolysis and induces plasma membrane internalization by down-regulating recycling. *J. Biol. Chem.* 289:16736–16747. doi:10.1074/jbc.M113.525782.

Lewis, M.J., B.J. Nichols, C. Prescianotto-Baschong, H. Riezman, and H.R. Pelham. 2000. Specific retrieval of the exocytic SNARE Snc1p from early yeast endosomes. *Mol. Biol. Cell*. 11:23–38.

Liu, K., Z. Hua, J.A. Nepute, and T.R. Graham. 2007. Yeast P4-ATPases Drs2p and Dnf1p are essential cargos of the NPFXD/Sla1p endocytic pathway. *Mol. Biol. Cell*. 18:487–500. doi:10.1091/mbc.E06-07-0592.

MacDonald, C., and R.C. Piper. 2015. Puromycin- and methotrexate-resistance cassettes and optimized Cre-recombinase expression plasmids for use in yeast. *Yeast*. 32:423–438. doi:10.1002/yea.3069.

MacDonald, C., and R.C. Piper. 2016. Cell surface recycling in yeast: mechanisms and machineries. *Biochem. Soc. Trans.* 44:474–478. doi:10.1042/BST20150263.

MacDonald, C., J.A. Payne, M. Aboian, W. Smith, D.J. Katzmann, and R.C. Piper. 2015. A family of tetraspans organizes cargo for sorting into multivesicular bodies. *Developmental Cell*. 33:328–342. doi:10.1016/j.devcel.2015.03.007.

MacGurn, J.A., P.-C. Hsu, M.B. Smolka, and S.D. Emr. 2011. TORC1 Regulates Endocytosis via Npr1-Mediated Phosphoinhibition of a Ubiquitin Ligase Adaptor. *Cell*. 147:1104–1117. doi:10.1016/j.cell.2011.09.054.

Martín, Y., Y.V. González, E. Cabrera, C. Rodríguez, and J.M. Siverio. 2011. Npr1 Ser/Thr protein kinase links nitrogen source quality and carbon availability with the yeast nitrate transporter (Ynt1) levels. *J. Biol. Chem.* 286:27225–27235. doi:10.1074/jbc.M111.265116.

Maxfield, F.R., and T.E. McGraw. 2004. Endocytic recycling. *Nat. Rev. Mol. Cell Biol.* 5:121–132. doi:10.1038/nrm1315.

McCullough, J., A.K. Clippinger, N. Talledge, M.L. Skowyra, M.G. Saunders, T.V. Naismith, L.A. Colf, P. Afonine, C. Arthur, W.I. Sundquist, P.I. Hanson, and A. Frost. 2015. Structure and membrane remodeling activity of ESCRT-III helical polymers. *Science*. 350:1548–1551. doi:10.1126/science.aad8305.

Merhi, A., and B. André. 2012. Internal amino acids promote Gap1 permease ubiquitylation via TORC1/Npr1/14-3-3-dependent control of the Bul arrestin-like adaptors. *Mol. Cell. Biol.* 32:4510–4522. doi:10.1128/MCB.00463-12.

Merwin, J.R., L.B. Bogar, S.B. Poggi, R.M. Fitch, A.W. Johnson, and D.E. Lycan. 2014. Genetic analysis of the ribosome biogenesis factor Ltv1 of Saccharomyces cerevisiae. *Genetics*. 198:1071–1085. doi:10.1534/genetics.114.168294.

Mioka, T., K. Fujimura-Kamada, and K. Tanaka. 2014. Asymmetric distribution of phosphatidylserine is generated in the absence of phospholipid flippases in Saccharomyces cerevisiae. *Microbiologyopen*. 3:803–821. doi:10.1002/mbo3.211.

Müller, M., O. Schmidt, M. Angelova, K. Faserl, S. Weys, L. Kremser, T. Pfaffenwimmer, T. Dalik, C. Kraft, Z. Trajanoski, H. Lindner, and D. Teis. 2015. The coordinated action of the MVB pathway and autophagy ensures cell survival during starvation. *eLife*. 4:e07736. doi:10.7554/eLife.07736.

Novick, P., C. Field, and R. Schekman. 1980. Identification of 23 complementation groups required for post-translational events in the yeast secretory pathway. *Cell*. 21:205–215. doi:10.1016/0092-8674(80)90128-2.

O'Donnell, A.F., R.R. McCartney, D.G. Chandrashekarappa, B.B. Zhang, J. Thorner, and M.C. Schmidt. 2015. 2-Deoxyglucose impairs Saccharomyces cerevisiae growth by stimulating Snf1-regulated and α-arrestin-mediated trafficking of hexose transporters 1 and 3. *Mol. Cell. Biol.* 35:939–955. doi:10.1128/MCB.01183-14.

Ohgaki, R., M. Matsushita, H. Kanazawa, S. Ogihara, D. Hoekstra, and S.C.D. van Ijzendoorn. 2010. The Na+/H+ exchanger NHE6 in the endosomal recycling system is involved in the development of apical bile canalicular surface domains in HepG2 cells. *Mol. Biol. Cell.* 21:1293–1304. doi:10.1091/mbc.E09-09-0767.

Panchaud, N., M.-P. Péli-Gulli, and C. De Virgilio. 2013a. Amino acid deprivation inhibits TORC1 through a GTPase-activating protein complex for the Rag family GTPase Gtr1. *Sci Signal*. 6:ra42–ra42. doi:10.1126/scisignal.2004112.

Panchaud, N., M.-P. Péli-Gulli, and C. De Virgilio. 2013b. SEACing the GAP that nEGOCiates TORC1 activation: evolutionary conservation of Rag GTPase regulation. *Cell Cycle*. 12:2948–2952. doi:10.4161/cc.26000.

Péli-Gulli, M.-P., A. Sardu, N. Panchaud, S. Raucci, and C. De Virgilio. 2015. Amino Acids Stimulate TORC1 through Lst4-Lst7, a GTPase-Activating Protein Complex for the Rag Family GTPase Gtr2. *Cell Rep*. 13:1–7. doi:10.1016/j.celrep.2015.08.059.

Pfannmüller, A., D. Wagner, C. Sieber, B. Schönig, M. Boeckstaens, A.M. Marini, and B. Tudzynski. 2015. The General Amino Acid Permease FfGap1 of Fusarium fujikuroi Is Sorted to the Vacuole in a Nitrogen-Dependent, but Npr1 Kinase-Independent Manner. *PLoS ONE*. 10:e0125487. doi:10.1371/journal.pone.0125487.

Piper, R.C., I. Dikic, and G.L. Lukacs. 2014. Ubiquitin-dependent sorting in endocytosis. *Cold Spring Harbor Perspectives in Biology*. 6:a016808. doi:10.1101/cshperspect.a016808.

Powis, K., and C. De Virgilio. 2016. Conserved regulators of Rag GTPases orchestrate amino acid-dependent TORC1 signaling. *Cell Discov*. 2:15049. doi:10.1038/celldisc.2015.49.

Powis, K., T. Zhang, N. Panchaud, R. Wang, C. De Virgilio, and J. Ding. 2015. Crystal structure of the Ego1-Ego2-Ego3 complex and its role in promoting Rag GTPase-dependent TORC1 signaling. *Cell Res.* 25:1043–1059. doi:10.1038/cr.2015.86.

Robinson, M., P.P. Poon, C. Schindler, L.E. Murray, R. Kama, G. Gabriely, R.A. Singer, A. Spang, G.C. Johnston, and J.E. Gerst. 2006. The Gcs1 Arf-GAP mediates Snc1,2 v-SNARE retrieval to the Golgi in yeast. *Mol. Biol. Cell*. 17:1845–1858. doi:10.1091/mbc.E05-09-0832.

Roth, A.F., and N.G. Davis. 1996. Ubiquitination of the yeast a-factor receptor. *J. Cell Biol.* 134:661–674.

Rue, S.M., S. Mattei, S. Saksena, and S.D. Emr. 2008. Novel Ist1-Did2 complex functions at a late step in multivesicular body sorting. *Mol. Biol. Cell*. 19:475–484. doi:10.1091/mbc.E07-07-0694.

Schäfer, T., B. Maco, E. Petfalski, D. Tollervey, B. Böttcher, and U. Aebi. 2006. Hrr25-dependent phosphorylation state regulates organization of the pre-40S subunit. *Nature*. 441:651–655. doi:10.1038/nature04840.

Schmidt, A., T. Beck, A. Koller, J. Kunz, and M.N. Hall. 1998. The TOR nutrient signalling pathway phosphorylates NPR1 and inhibits turnover of the tryptophan permease. *EMBO J.* 17:6924–6931. doi:10.1093/emboj/17.23.6924.

Seaman, M.N., J.M. McCaffery, and S.D. Emr. 1998. A membrane coat complex essential for endosome-to-Golgi retrograde transport in yeast. *J. Cell Biol.* 142:665–681.

Sebastian, T.T., R.D. Baldridge, P. Xu, and T.R. Graham. 2012. Phospholipid flippases: building asymmetric membranes and transport vesicles. *Biochim. Biophys. Acta*. 1821:1068–1077. doi:10.1016/j.bbalip.2011.12.007.

Seiser, R.M., A.E. Sundberg, B.J. Wollam, P. Zobel-Thropp, K. Baldwin, M.D. Spector, and D.E. Lycan. 2006. Ltv1 is required for efficient nuclear export of the ribosomal small subunit in Saccharomyces cerevisiae. *Genetics*. 174:679–691. doi:10.1534/genetics.106.062117.

Sheff, D.R., E.A. Daro, M. Hull, and I. Mellman. 1999. The receptor recycling pathway contains two distinct populations of early

endosomes with different sorting functions. *J. Cell Biol.* 145:123–139.

Shestakova, A., A. Hanono, S. Drosner, M. Curtiss, B.A. Davies, D.J. Katzmann, and M. Babst. 2010. Assembly of the AAA ATPase Vps4 on ESCRT-III. *Mol. Biol. Cell*. 21:1059–1071. doi:10.1091/mbc.E09-07-0572.

Shi, Y., C.J. Stefan, S.M. Rue, D. Teis, and S.D. Emr. 2011. Two novel WD40 domain-containing proteins, Ere1 and Ere2, function in the retromer-mediated endosomal recycling pathway. *Mol. Biol. Cell*. 22:4093–4107. doi:10.1091/mbc.E11-05-0440.

Snider, M.D., and O.C. Rogers. 1985. Intracellular movement of cell surface receptors after endocytosis: resialylation of asialo-transferrin receptor in human erythroleukemia cells. *J. Cell Biol.* 100:826–834.

Stringer, D.K., and R.C. Piper. 2011. A single ubiquitin is sufficient for cargo protein entry into MVBs in the absence of ESCRT ubiquitination. *J. Cell Biol.* 192:229–242. doi:10.1083/jcb.201008121.

Tanaka, K., K. Fujimura-Kamada, and T. Yamamoto. 2011. Functions of phospholipid flippases. *Journal of Biochemistry*. 149:131–143. doi:10.1093/jb/mvq140.

Tanner, L.I., and G.E. Lienhard. 1987. Insulin elicits a redistribution of transferrin receptors in 3T3-L1 adipocytes through an increase in the rate constant for receptor externalization. *Journal of Biological Chemistry*. 262:8975–8980.

Urbanowski, J.L., and R.C. Piper. 1999. The Iron Transporter Fth1p Forms a Complex with the Fet5 Iron Oxidase and Resides on the Vacuolar Membrane. *J. Biol. Chem.* 274:38061–38070. doi:10.1074/jbc.274.53.38061.

Valbuena, N., K.-L. Guan, and S. Moreno. 2012. The Vam6 and Gtr1-Gtr2 pathway activates TORC1 in response to amino acids in fission yeast. *J. Cell. Sci.* 125:1920–1928. doi:10.1242/jcs.094219.

Wiederkehr, A., K.D. Meier, and H. Riezman. 2001. Identification and characterization of Saccharomyces cerevisiae mutants defective in fluid- phase endocytosis. *Yeast*. 18:759–773. doi:10.1002/yea.726.

Wiederkehr, A., S. Avaro, C. Prescianotto-Baschong, R. Haguenauer-Tsapis, and H. Riezman. 2000. The F-box protein Rcy1p is involved in endocytic membrane traffic and recycling out of an early endosome in Saccharomyces cerevisiae. *J. Cell Biol.* 149:397–410.

Winzeler, E.A. 1999. Functional Characterization of the S. cerevisiae Genome by Gene Deletion and Parallel Analysis. *Science*. 285:901–906. doi:10.1126/science.285.5429.901.

Winzeler, E.A., D.D. Shoemaker, A. Astromoff, H. Liang, K. Anderson, B. Andre, R. Bangham, R. Benito, J.D. Boeke, H. Bussey, A.M. Chu, C. Connelly, K. Davis, F. Dietrich, S.W. Dow, M. El Bakkoury, F. Foury, S.H. Friend, E. Gentalen, G. Giaever, J.H. Hegemann, T. Jones, M. Laub, H. Liao, N. Liebundguth, D.J. Lockhart, A. Lucau-Danila, M. Lussier, N. M'Rabet, P. Menard, M. Mittmann, C. Pai, C. Rebischung, J.L. Revuelta, L. Riles, C.J. Roberts, P. Ross-MacDonald, B. Scherens, M. Snyder, S. Sookhai-Mahadeo, R.K. Storms, S. Véronneau, M. Voet, G. Volckaert, T.R. Ward, R. Wysocki, G.S. Yen, K. Yu, K. Zimmermann, P. Philippsen, M. Johnston, and R.W. Davis. 1999. Functional characterization of the S. cerevisiae genome by gene deletion and parallel analysis. *Science*. 285:901–906.

Xu, P., R.D. Baldridge, R.J. Chi, C.G. Burd, and T.R. Graham. 2013. Phosphatidylserine flipping enhances membrane curvature and negative charge required for vesicular transport. *J. Cell Biol.* 202:875–886. doi:10.1083/jcb.201305094.

Materials & Methods

Reagents

Yeast strains and plasmids used in this study are listed in **Tables S3** and **S4**. Both Sec1 and Sec7 are essential for growth and the efficacy of the temperature-sensitive cells used for experiments was verified by absence of growth at 37°C (**Fig. 1D**). Plasmids expressing nucleotide-bound locked mutants of Gtr1 and Gtr2 were: $Gtr1^{GTP}$, Gtr1-Q65L(active); $Gtr2^{GTP}$, Gtr2-Q66L(inactive); $Gtr1^{GDP}$, Gtr1-S20L(inactive); $Gtr2^{GDP}$, Gtr2-S23L(active), as described previously (Binda et al., 2009).

Cell culture conditions

Standard yeast extract peptone dextrose (YPD) rich medium (2% glucose, 2% peptone, 1% yeast extract) and synthetic complete (SC) minimal medium (2% glucose, yeast nitrogen base; Research Products International, Mount Prospect, IL, USA), lacking appropriate amino acids and bases for plasmid selection were used. Geneticin (G418), used at a concentration of 250 µg/ml and methotrexate (Sigma-Aldrich, St. Louis, MO, USA), used as described (MacDonald and Piper, 2015), were utilized for selection of yeast integrant strains. For genetic screening the MAT alpha haploid deletion library (Winzeler et al., 1999) was purchased from Dharmacon Inc. Expression of plasmids containing the *CUP1* promoter was generally induced by the addition of 10-50 µM copper chloride to the media. Media enriched in **a**-factor was achieved by culturing BY4741 MAT **A** cells transformed with overexpression plasmid pKK16, to increase expression of the Mating pheromone **a**-factor *MFA1* and the peptide export transporter *STE6* genes (Kuchler et al., 1989), to provide robust production and secretion, respectively, of **a**-factor. Yeast cells were then removed by centrifugation and the media used directly to induce Ste3 internalization. Cells were routinely harvested from cultures grown to early / mid-log phase (OD_{600} = 0.5 - 1.0), or late-log phase (OD_{600} = 2.0), where labeled, prior to fluorescence microscopy. For leucine starvation, *leu2* mutant cells (BY4742 background) were grown in minimal media containing leucine, pelleted and resuspended in minimal media lacking leucine for 15 min or 30 min prior to assay.

Transformation of yeast deletion library

Transformation of the yeast gene deletion library was performed according to a high-throughput transformation protocol (Gietz and Schiestl, 2007). Briefly, yeast strains were grown in 96 well plates, pelleted by centrifugation, and incubated for 12 hours at 30°C in 100 µls of 50 mM Tris pH 8.0, 100 mM LiAc, 0.5mM EDTA, 50% PEG, 50 ng/µl plasmid expressing Ste3-GFP-Dub from a low copy (*CEN*-based pRS316) plasmid under the control of the *STE3* promoter. Cells were pelleted, grown and maintained in minimal media lacking Uracil upon dilution in several new 96 well plates. Cells were grown overnight in minimal media, pelleted, and resuspended in batches of 24 in minimal media prior to imaging by fluorescence microscopy.

Immunoblotting

Yeast cells harvested at mid-log phase were subjected to alkali treatment (0.2 N NaOH) for 3 minutes followed by resuspension in 50 mM Tris,HCl (pH 6.8), 5% SDS, 10% glycerol, and 8 M urea, to prepare whole cell lysates. Proteins resolved by SDS-PAGE were immunodetected with monoclonal antibodies raised against the HA epitope (HA.11; Biolegend, SanDiego, CA), Carboxypeptidase Y (10A5B5; Thermo Fisher, Waltham, MA), Pgk1 (22C5D8; Thermo Fisher, Waltham, MA) and polyclonal antibodies that recognize GFP (Urbanowski and Piper, 1999).

Fluorescence Microscopy

Yeast cells were concentrated and resuspended in minimal media or kill buffer (100 mM Tris.HCl (pH 8.0), 0.2% (w/v) NaN_3 and NaF_3), prior to fluorescence microscopy. GFP, mCherry, mStrawberry, and FM4-64 signals were imaged using a BX60 epifluorescence microscope (Olympus) using a 100x objective lens with a Numerical Aperture = 1.4. Images were captured at room temperature with a cooled charge-coupled camera (Orca R2; Hamamatsu Photonics) using iVision-Mac software (Biovision Technology). Mup1-mCherry-Ub localization was recorded following a 1-hr incubation in minimal media containing 20 µg/ml methionine and 5 µM copper chloride. For localization with FM4-64 (Molecular Probes™, Eugene, OR) labeled early endosomes, cells grown in minimal media were pelleted and

resuspended in 40 µM FM4-64 in YPD media, and incubated for 2 min at 22°C. FM4-64 was added from a 400 µM stock containing 10% DMSO to yield a final labeling concentration of 1% DMSO. Cells were centrifuged and resuspended 3 times in 0°C kill buffer, and resuspended in kill buffer and stored on ice prior to microscopy. Labeling of temperature sensitive mutants (*sec1-1* and *sec7-1*) was accomplished by labeling cells in 40 µM FM4-64 for 2 min at 22°C in YPD. Cells were centrifuged and resuspended in minimal media prewarmed to either 22°C or 37°C, incubated at their respective temperatures for an additional 15 min before 3 washes in 0° kill buffer and storage on ice before visualization microscopy. For localization with FM4-64 labeled vacuoles, rich media containing 40 µM FM4-64 was incubated for 10 min at room temperature, followed by 3x washes with minimal media and further incubation with minimal media for 1-hour. For localization of Mup1-GFP, Mup1-GFP was expressed from the low copy *LEU2* based plasmid (pPL4070), unless in leucine starvation experiments from the *URA3*-based (pPL4023) plasmid. Cells were grown to mid-log phase in minimal media lacking methionine.

FM4-64 efflux assay

To measure FM4-64 efflux under standard conditions, cells were grown in YPD to mid-log phase (OD_{600} =1), pelleted and resuspended in 200 µl YPD media containing 40 µM FM4-64 and incubated at 22°C for 10 min. Cells were transferred to a 0°C water bath for initial chilling and then subjected to 3 washes (5 min each) in ice-cold buffer followed by pelleting in a cold centrifuge. Cells were stored in a 0°C ice-bath at a concentrated density prior to addition (2000x) pre-warmed media at 22°C. FM4-64 fluorescence was measured by flow cytometry using a Becton Dickinson LSR II. Binned averages of approximately 100,000 cells in 1-min increments were used to plot results. To measure FM4-64 efflux in *sec1-1* and *sec7-1* temperature-sensitive mutants, cells were grown in YPD at 22°C, pelleted, and resuspended in 200 µl YPD media containing 40 µM FM4-64 and incubated for 9 min at 22°C. Cells were washed 3 times in cold minimal media as in the standard protocol above, and then resuspended in 0°C minimal media to a concentration of 400 million cells/100 µls of cold minimal media and stored in a glass tubes immersed in a 0°C water bath. 15 µl of the cell suspension was then diluted in prewarmed tubes containing 2 mls of pre-warmed media at 22°C or 37°C. Temperature was maintained in an insulated chamber comprised of a metal cylinder immersed in a beaker containing water at 37°C or 22°C during efflux measurements taken by flow cytometry.

Limited Tryptophan growth assay

Cells were grown to mid-log phase, equivalent volumes harvested and used to create a serial dilution (1:9) prior to plating on SC media plates containing replete (40 µg/ml), moderate (5 µg/ml) or low (2.5 µg/ml) Tryptophan concentrations. Wild-type parental strain (SEY6210) control cultures were included on each plate. Plates were then incubated for 48 hours at 30°C and growth documented.

Figure legends

Figure 1. FM4-64 follows a Golgi-independent route from early endosomes to the plasma membrane.
(A) FM4-64 efflux measurements and (**B**) localization of remaining dye from wild-type and *vps4*Δ cells after 9 min uptake of FM4-64 at 25°C followed by 0 or 15 min chase prior to the assay.
(**C**) FM4-64 efflux in *sec1-1* and *sec7-1* temperature-sensitive (*ts*) cells performed at 22°C or 37°C (upper), with growth phenotype of *ts* mutants confirmed (lower).
(**D**) Colocalization of GFP-Snc1 with FM4-64 labeled endosomes following 10 min uptake assessed in *ts* mutants at 22°C or 37°C. Bar, 5 μm.

Figure 2. Various cargoes utilize an Rcy1-dependent recycling route.
(**A**) Accumulation of FM4-64 at indicated chase times in wild-type and *rcy1*Δ cells, micrographs were normalized across the series.
(**B**) FM4-64 efflux in indicated mutants.
(**C**) Mup1-GFP localization in wild-type and *rcy1*Δ grown to mid-log phase.
(**D**) Growth assays in wild-type and *rcy1*Δ cells carrying the *trp1* mutation using indicated concentrations of Trp.
(**E**) Wild-type cells expressing either Ste3-GFP or GFP-Snc1 were grown to mid- and late-log phase followed by fluorescence microscopy.
(**F**) Cartography of endocytic pathway: after internalization, cargo enters the Vps4-dependent MVB / degradation pathway or returns from early endosomes or late endosomes to the cell surface via the Golgi / TGN along routes that require Sec7 and Sec1. Cargo such as FM4-64 requires Rcy1 and Sec1, but not Sec7, to return to the plasma membrane. Bar, 5 μm.

Figure 3. A synthetic reporter that follows an Rcy1-dependent EE>PM route.
(**A**) Ste3-GFP-DUb, comprised of the Ste3 GPCR fused to GFP and the catalytic domain of the UL36 deubiquitinating enzyme (DUb), designed to be at the cell surface in wild-type cells and endosomes in recycling mutants.
(**B**) Localization of Ste3-GFP-DUb in wild-type and *rcy1*Δ cells or *sec1-1(ts)* and *sec7-1(ts)* cells grown at 22°C and 37°C.
(**C**) Immunoblot of vacuolar-processed GFP cleaved from Ste3-GFP-DUb or Ste3-GFP expressed in wild-type and *pep4*Δ cells.
(**D**) Ste3-GFP-DUb localization at mid- and late-log phase.
(**E**) Localization of Ste3-GFP and Ste3-GFP-DUb in labeled cells grown in media enriched with **a**-factor.
(**F**) Ste3-GFP-DUb expressed in indicated mutants colocalized with FM4-64 chased for 2 mins or (**G**) Mup1-RFP-Ub in the presence on 20 μg/nl methionine. Bar, 5 μm.

Figure 4. Genetic screen reveals mutants defective in EE>PM recycling.
Viable yeast deletion mutants (BY4742-derived) were screened visually for altered localization of plasmid-expressed Ste3-GFP-DUb.
(**A**) Mutants were imaged after growth to mid-log phase under identical conditions. Indicated mutants are color-coded: Wild-type (orange); *rcy1*Δ (red); *ist1*Δ and *nhx1*Δ (green); *gtr1*Δ, *gtr2*Δ, *vam6*Δ and *ltv1*Δ (blue).
(**B**) Summary of FM4-64 efflux assays from mutants plotted as the percentage fluorescence loss after 10-min chase.
(**C**) Summary of growth defects in low tryptophan of mutants made in *trp1* auxotrophic (SEY6210-derived) parental strain. Bar, 5 μm.

Figure 5. Gtr1/Gtr2 control of EE>PM recycling is mediated through Vam6.
(**A**) Model for how Gtr1(GTP-bound) / Gtr2(GDP-bound) heterodimer localizes to the vacuolar membrane via the EGO complex to activate TORC1. Gtr1 is activated by the GEF Vam6, that senses leucine via the leucyl-tRNA synthetase, Cdc60. Vam6, Gtr1, Gtr2, are also required for recycling from early endosomes and work through Ltv1.

(**B**) Localization of Ste3-GFP-DUb in the indicated mutant cells counter-labeled with FM4-64 for 60 min or (**C**) 2-min.
(**D**) Efflux of FM4-64 in wild-type cells and *gtr1*Δ, *gtr2*Δ, *ltv1*Δ and *vam6*Δ cells carrying vector alone, or plasmids expressing Vam6, Gtr1, Gtr2, or Gtr1 and Gtr2 mutants locked in nucleotide-bound forms, $Gtr1^{GTP}$, $Gtr1^{GDP}$, $Gtr2^{GDP}$ or $Gtr2^{GTP}$. Bar, 5 μm.

Figure 6. The Vam6-Gtr1/Gtr2-Ltv1 pathway controls recycling independent of TORC1.
(**A**) Ste3-GFP-DUb localized with FM4-64 following a 60-min chase period in minimal media lacking dye.
(**B**) FM4-64 efflux of indicated mutants after 10 min.
(**C**) Experimental framework for tracing how the multifunctional proteins Vam6, Gtr1/Gtr2, and Ltv1 work together to control recycling rather than through their other known functions in endosomal fusion (Vam6, as part of the HOPS complex) TORC1 function (Gtr1/Gtr2, stimulators of TORC1 via the Ego Complex) and ribosomal biogenesis (Ltv1, as a regulator of pre-40S riborsome processing). Bar, 5 μm.

Figure 7. The recycling-specific Rag GTPase interactor Ltv1 controls recycling.
(**A**) Ltv1 chimeras from *Saccharomyces cerevisiae* (grey; *Sc*) and *Cylindrobasidium torrendii* (blue; *Ct*) with Rps3 and Rps20 binding sites and phosphomimetic Hrr1 phosphorylation sites shown.
(**B**) FM4-64 efflux of *ltv1*Δ cells expressing the indicated Ltv1 chimeras.
(**C**) Growth at 30°C and 18°C of the *ltv1*Δ cells expressing chimeras.
(**D**) Expression levels of HA-tagged chimeras estimated by western blotting using anti-CPY as a loading control.
(**E**) Wild-type and active nucleotide-bound mutant Rag GTPases tagged with mCherry (RFP) and Ltv1-GFP localized in wild-type cells.
(**F**) Rag GTPases colocalized (arrowheads) with Ltv1-GFP (upper) and Ste3-GFP-DUb (lower) in *nhx1*Δ cells.
(**G**) Ste3-GFP-Dub and Gtr1-RFP were localized in *nhx1*Δ *ltv1*Δ and *drs2*Δ mutants. Bar, 5 μm.

Figure 8. The Vam6-Gtr1/Gtr2-Ltv1 pathway control recycling in response to leucine starvation.
(**A**) Localization of Ste3-GFP-Ub after acute leucine starvation.
(**B**) FM4-64 efflux after acute leucine starvation in wild-type cells alone or cells expressing $Gtr1^{GTP}$.
(**C**) Mup1-GFP was localized in indicated mutants grown to mid-log phase.
(**D**) Localization of Mup1-GFP in wild-type and *ltv1*Δ cells in replete media (+Leu), following 30-min leucine starvation (-Leu), or after 30 min Rapamycin (200 ng/ml) treatment. Bar, 5 μm.

Supplemental Figure legends

Figure S1: Secondary screens used to validate mutants in the recycling pathway.
(**a**) The proteins implicated in the EE>PM recycling pathway were analyzed using STRING pathway software (version 10; Szklarczyk *et al*. Nucleic Acids Research, 2015,) and clustered in modules based on their protein-protein interactions and molecular functions .
(**b**) Transformants positively identified from the initial Ste3-GFP-DUb reporter localization screen were struck onto 5-FOA media to remove the *URA3*-marked reporter plasmid before strains were genotyped. Validated strains were then used to perform FM4-64 efflux assays, by labeling cells for 10 minutes at room temperature, washing in cold media and then rate of FM4-64 secretion measured by flow cytometry (FM4-64 fluorescence recorded for approximately 1 million cells per sample) over a 10-minute chase period at 22ºC. Depicted is the recycling kinetics for each strain with averaged wild-type data included in each graph for comparison.
(**c**) Schematic diagram to show endosomal trafficking of Tat2 in Tryptophan auxotroph (Trp^-) SEY6210 yeast strains harboring deletions of indicated genes. Under wild-type conditions the recycling pathway provides ample Tat2 at the surface to maintain growth, even in poor Tryptophan (Trp) conditions (left). However, mutant cells defective for recycling Tat2 back to the plasma membrane mainly route the permease to the multivesicular body pathway, where it is degraded in the vacuole. The reduced levels of Tat2 at the surface of Trp auxotrophs cannot uptake sufficient Trp to support efficient growth, resulting in a defect when Trp levels are restricted.
(**d**) Genes identified as recycling mutants were deleted in the SEY6210 (Trp^-) background strain. Wild-type cells and mutants were grown to mid-log phase, washed in water and serially diluted (1:9) on plates of replete (40 µg/ml) and restricted (5 µg /ml and 2.5 µg /ml) Trp levels.

Figure S2. Endosomal proteins that control EE>PM recycling.
(**a**) Localization of Mup1-GFP and Ste3-GFP-DUb in the indicated mutants grown in minimal media lacking methionine to mid-log phase (OD_{600}= 1.0).
(**b**). Localization in the indicated mutants of Ste3-GFP-DUb and Cos5-mCherry, a heavily ubiquitinated membrane proteins that sorts efficiently into the MVB pathway (upper), or a 2 min pulse of FM4-64 to mark early endosomes (lower).
(c) Localization of Ste3-GFP-DUB and Cos5-mCherry (a ubiquitinated protein that follows the biosynthetic pathway from the TGN to late endosomes where it undergoes MVB sorting) in *nhx1*Δ *vps4*Δ double mutant cells. Note, Ste3-GFP-DUb accumulates in different intracellular punctate structures than does Cos5-mCherry, which occupies a compartment that is characteristic of the class E compartment large late endosomes that accumulate in *vps4*Δ mutants.
(**d**) FM4-64 efflux assays were performed in *vps4*Δ mutants or *ist1*Δ cells transformed with an empty vector control (vector) or plasmids expressing wild-type Ist1 (WT) or a mutant Ist1 expressing only residues 1-287 (ΔMIM), which lacks the C-terminal **M**IT-**i**nteraction **m**otif (MIM) required to bind Vps4.
(**e**) Levels of Ist1 were compared in different recycling mutants by immunoblot analysis, with loading controls using antibodies raised against CPY and Rsp5. Bar, 5 µm.

Figure S3: TORC1-indepedent recycling relies on specific features of Ltv1.
(a, b) FM4-64 efflux profiles for indicated mutants or wild-type (WT) cells treated with 200 ng/ml Rapamycin (+) or DMSO (-) control. A subset of these data are summarized in bar graph form in Figure 6B.
(c) Localization of Ste3-GFP-DUb in indicated strains after labeling of FM4-64 for 30 minutes followed by a 60 minute chase period in dye-free minimal media.
(d) Plasmids expressing Ltv1 from *Saccharomyces cerevisiae* were created with mutant (Serine to Glutamate) Hrr25 phosphorylation sites (dark grey). Chimeras retaining the *S. cerevisiae* Rps3 and Rps20 binding sequences, including mutant phosphorylation sites, were created from Ltv1 sequences from different species (light grey), including: *Octopus vulgaris*, *Citrus clementina*, *Mus musculus*, *Cylindrobasidium torrendii*, *Calocera viscosa*, *Trametes versicolor*.
(**e**) Mutant *ltv1*Δ cells were transformed with plasmids expressing Ltv1 chimeras described in (**d**) and grown to mid-log phase before equivalent volumes were harvested, resuspended in water and plated

with a 10-fold serial dilution on SC-Ura-Met plates. Plates were then incubated at 30°C and 18°C.
(**f**) FM4-64 efflux assays were performed in mutant *ltv1*Δ cells expressing different chimeras that either complemented the growth defect of *ltv1*Δ cells (upper) or that failed to complement growth *ltv1*Δ growth defects (lower).
(**g**) FM4-64 efflux assays were performed in Wild-type cells, mutant *ltv1*Δ single null mutants, *nhx1*Δ single null mutants, or *nhx1*Δ *ltv1*Δ double null mutants.

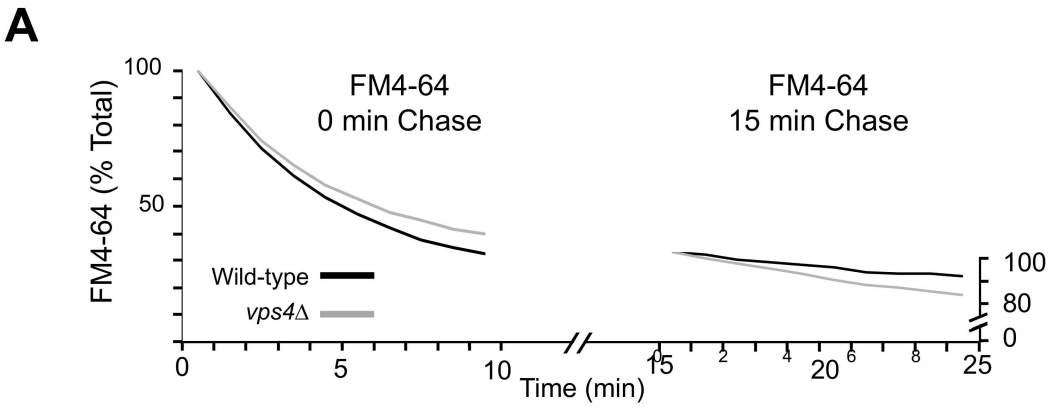
A
FM4-64 (% Total)
100
50
FM4-64
0 min Chase
FM4-64
15 min Chase
Wild-type
vps4Δ
0
5
10
15
20
25
100
80
0
Time (min)

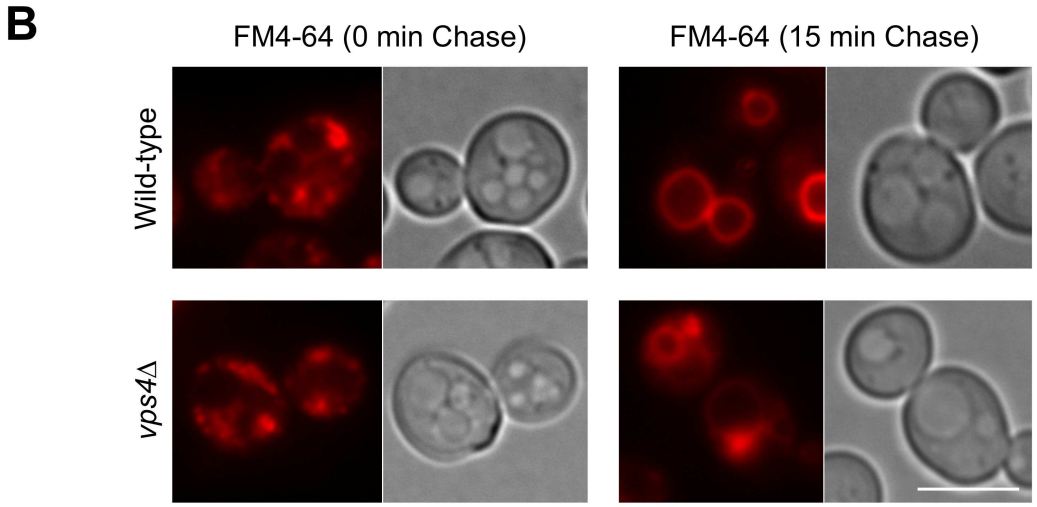
B
FM4-64 (0 min Chase)
FM4-64 (15 min Chase)
Wild-type
vps4Δ

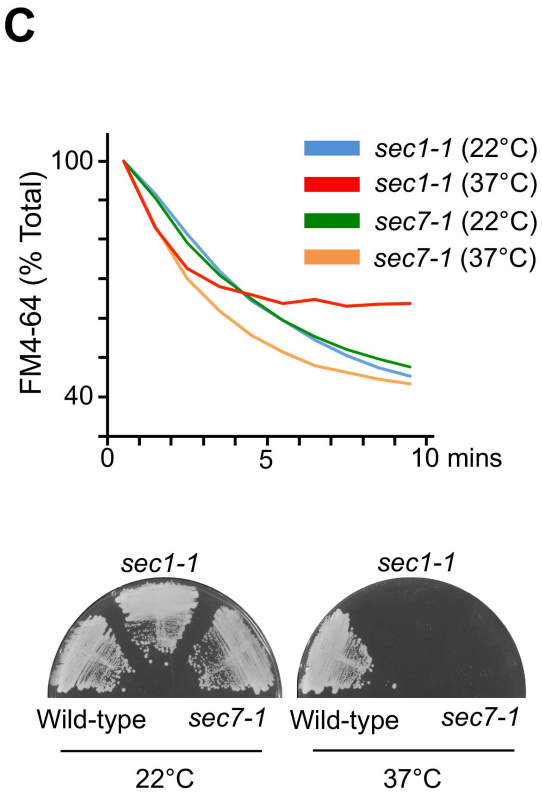
C
FM4-64 (% Total)
100
40
0
5
10 mins
sec1-1 (22°C)
sec1-1 (37°C)
sec7-1 (22°C)
sec7-1 (37°C)
sec1-1
sec1-1
Wild-type
sec7-1
Wild-type
sec7-1
22°C
37°C

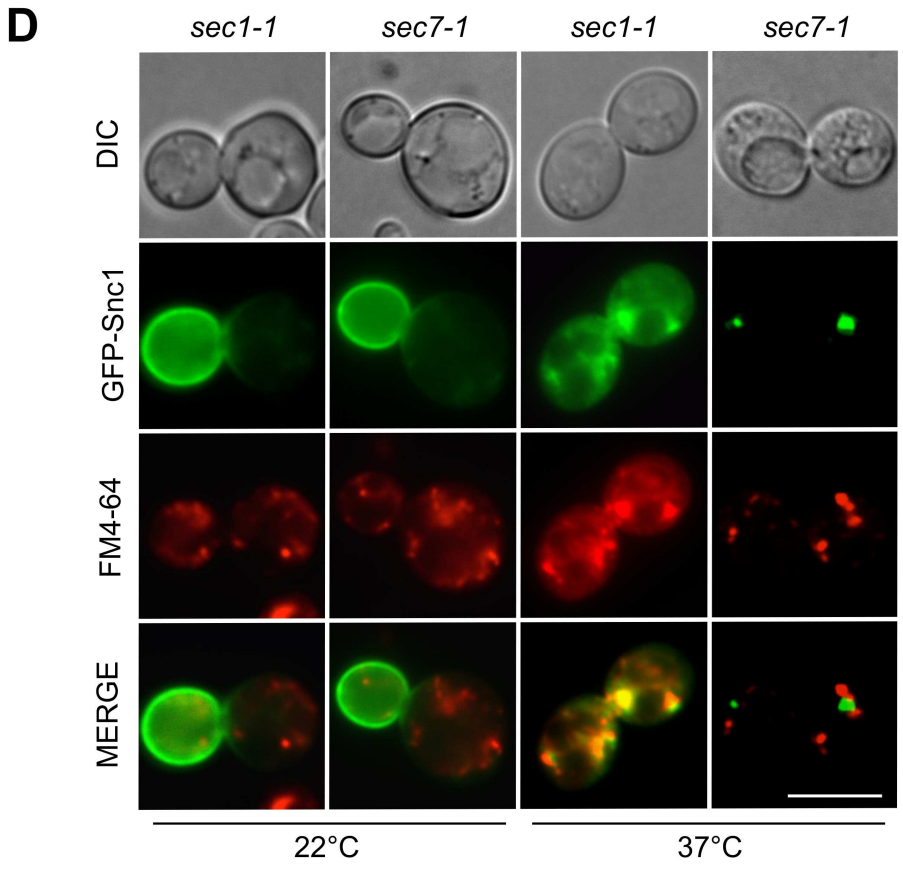
D
sec1-1
sec7-1
sec1-1
sec7-1
DIC
GFP-Snc1
FM4-64
MERGE
22°C
37°C

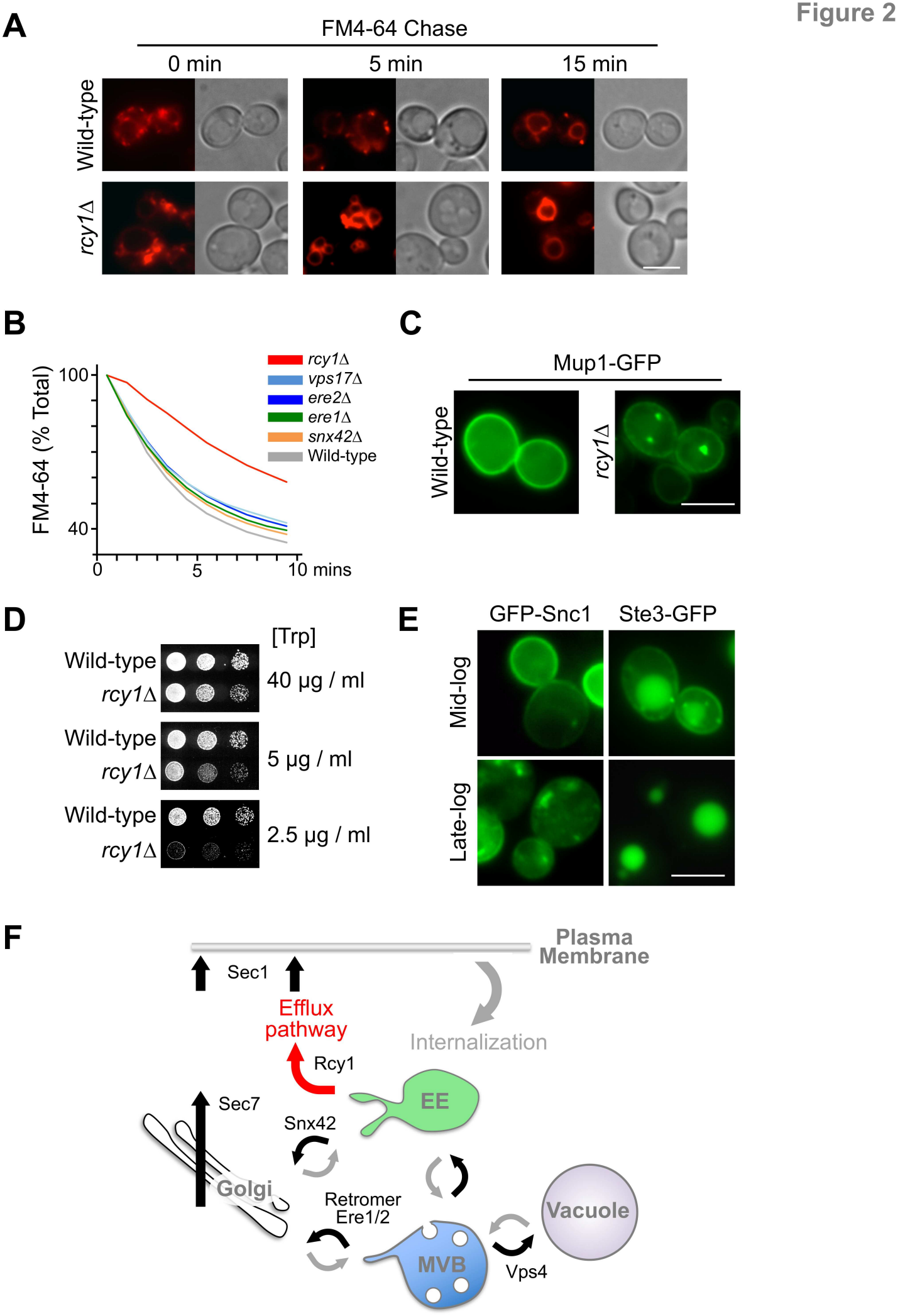
A
FM4-64 Chase
0 min
5 min
15 min
Wild-type
rcy1Δ
B
FM4-64 (% Total)
100
40
0
5
10 mins
rcy1Δ
vps17Δ
ere2Δ
ere1Δ
snx42Δ
Wild-type
C
Mup1-GFP
Wild-type
rcy1Δ
D
[Trp]
Wild-type
rcy1Δ
40 µg / ml
5 µg / ml
2.5 µg / ml
E
GFP-Snc1
Ste3-GFP
Mid-log
Late-log
F
Plasma Membrane
Sec1
Efflux pathway
Rcy1
Internalization
EE
Sec7
Snx42
Golgi
Retromer Ere1/2
MVB
Vps4
Vacuole

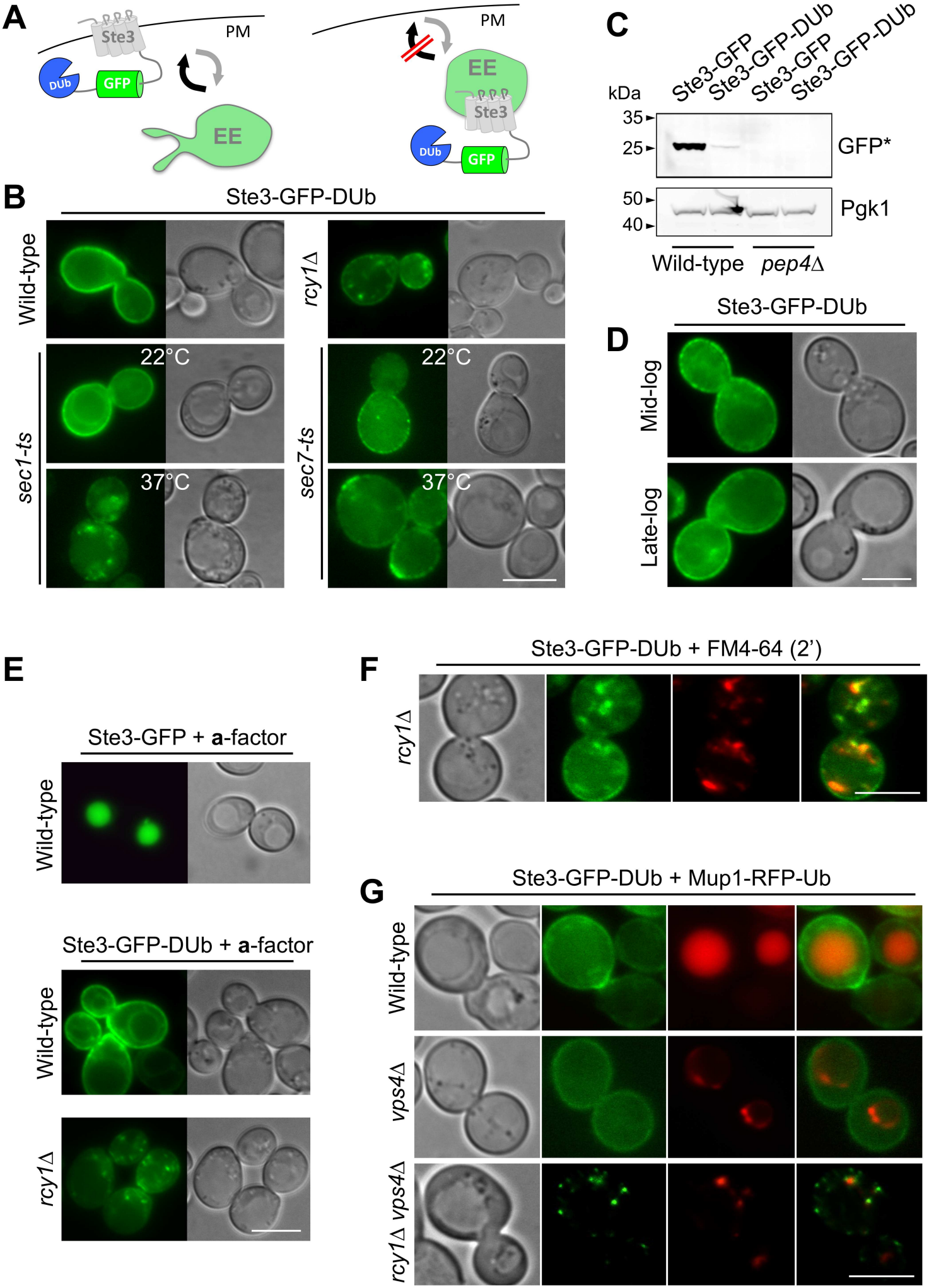
A
Ste3
PM
DUb
GFP
EE
PM
EE
Ste3
DUb
GFP
B
Ste3-GFP-DUb
Wild-type
rcy1Δ
sec1-ts
sec7-ts
22°C
37°C
22°C
37°C
C
Ste3-GFP
Ste3-GFP-DUb
Ste3-GFP
Ste3-GFP-DUb
kDa
35
25
GFP*
50
40
Pgk1
Wild-type
pep4Δ
D
Ste3-GFP-DUb
Mid-log
Late-log
E
Ste3-GFP + a-factor
Wild-type
Ste3-GFP-DUb + a-factor
Wild-type
rcy1Δ
F
Ste3-GFP-DUb + FM4-64 (2')
rcy1Δ
G
Ste3-GFP-DUb + Mup1-RFP-Ub
Wild-type
vps4Δ
rcy1Δ vps4Δ

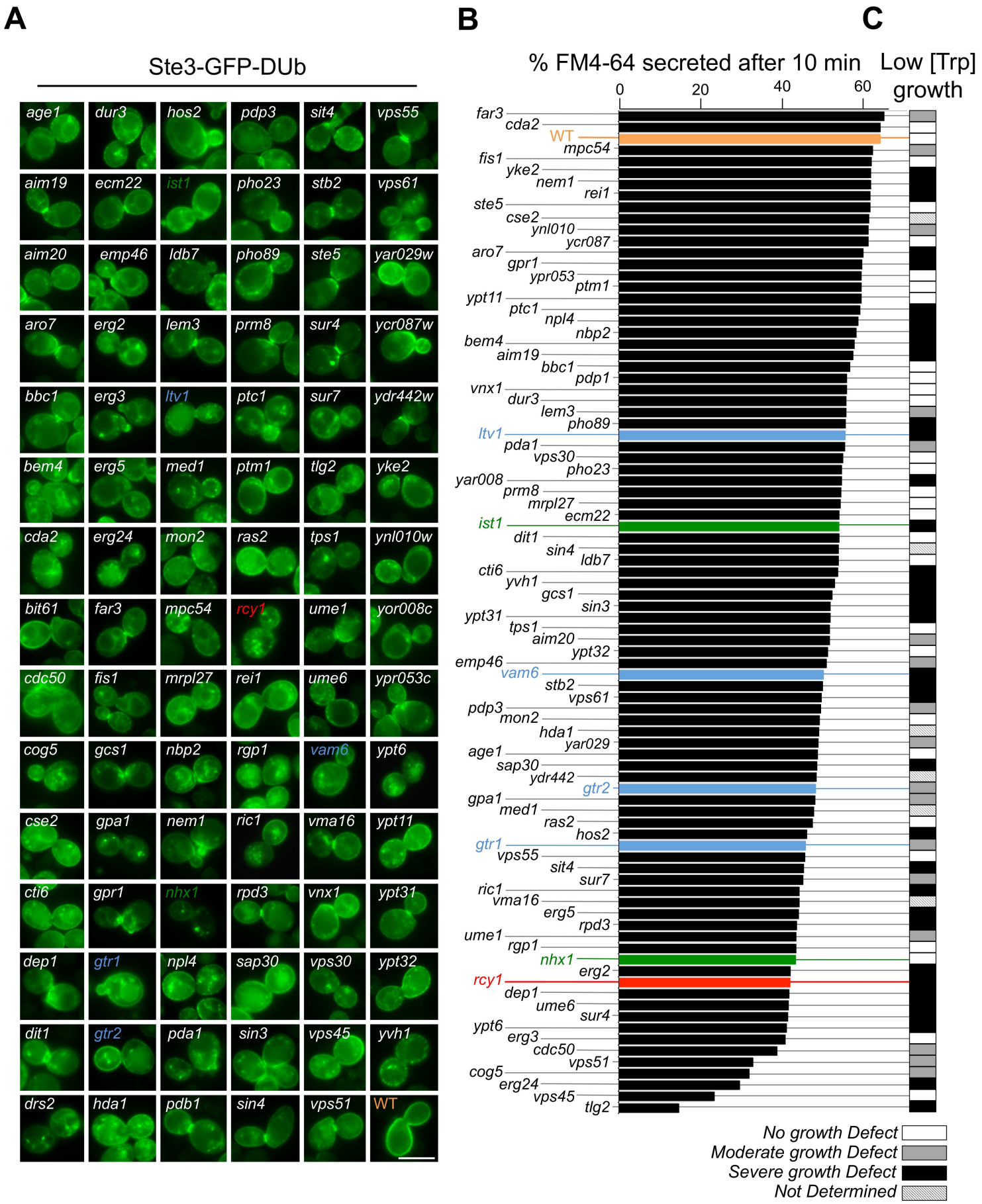
A
Ste3-GFP-DUb
age1 dur3 hos2 pdp3 sit4 vps55
aim19 ecm22 ist1 pho23 stb2 vps61
aim20 emp46 ldb7 pho89 ste5 yar029w
aro7 erg2 lem3 prm8 sur4 ycr087w
bbc1 erg3 ltv1 ptc1 sur7 ydr442w
bem4 erg5 med1 ptm1 tlg2 yke2
cda2 erg24 mon2 ras2 tps1 ynl010w
bit61 far3 mpc54 rcy1 ume1 yor008c
cdc50 fis1 mrpl27 rei1 ume6 ypr053c
cog5 gcs1 nbp2 rgp1 vam6 ypt6
cse2 gpa1 nem1 ric1 vma16 ypt11
cti6 gpr1 nhx1 rpd3 vnx1 ypt31
dep1 gtr1 npl4 sap30 vps30 ypt32
dit1 gtr2 pda1 sin3 vps45 yvh1
drs2 hda1 pdb1 sin4 vps51 WT
B
% FM4-64 secreted after 10 min
0
20
40
60
C
Low [Trp] growth
far3 cda2 WT mpc54 fis1 yke2 nem1 rei1 ste5 cse2 ynl010 ycr087 aro7 gpr1 ypr053 ptm1 ypt11 ptc1 npl4 nbp2 bem4 aim19 bbc1 pdp1 vnx1 dur3 lem3 pho89 ltv1 pda1 vps30 pho23 yar008 prm8 mrpl27 ecm22 ist1 dit1 sin4 ldb7 cti6 yvh1 gcs1 sin3 ypt31 tps1 aim20 ypt32 emp46 vam6 stb2 vps61 pdp3 mon2 hda1 yar029 age1 sap30 ydr442 gtr2 gpa1 med1 ras2 hos2 gtr1 vps55 sit4 sur7 ric1 vma16 erg5 rpd3 ume1 rgp1 nhx1 erg2 rcy1 dep1 ume6 sur4 ypt6 erg3 cdc50 vps51 cog5 erg24 vps45 tlg2
No growth Defect
Moderate growth Defect
Severe growth Defect
Not Determined

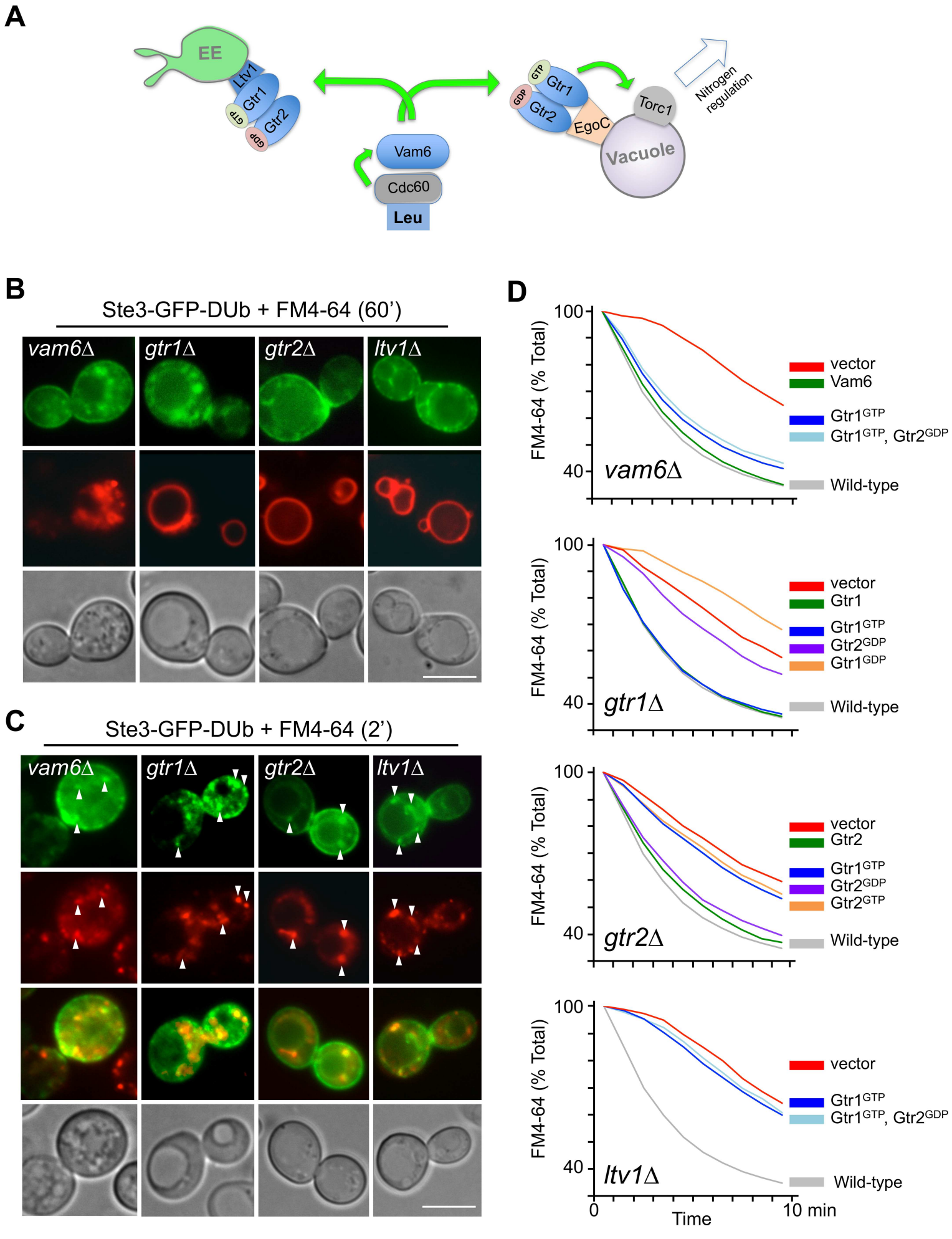
A
EE
Ltv1
Gtr1
Gtr2
GTP
GDP
Vam6
Cdc60
Leu
GTP
Gtr1
GDP
Gtr2
EgoC
Torc1
Vacuole
Nitrogen regulation
B
Ste3-GFP-DUb + FM4-64 (60')
vam6Δ
gtr1Δ
gtr2Δ
ltv1Δ
C
Ste3-GFP-DUb + FM4-64 (2')
vam6Δ
gtr1Δ
gtr2Δ
ltv1Δ
D
FM4-64 (% Total)
100
40
vam6Δ
vector
Vam6
Gtr1GTP
Gtr1GTP, Gtr2GDP
Wild-type
gtr1Δ
vector
Gtr1
Gtr1GTP
Gtr2GDP
Gtr1GDP
Wild-type
gtr2Δ
vector
Gtr2
Gtr1GTP
Gtr2GDP
Gtr2GTP
Wild-type
ltv1Δ
vector
Gtr1GTP
Gtr1GTP, Gtr2GDP
Wild-type
0
Time
10 min

A

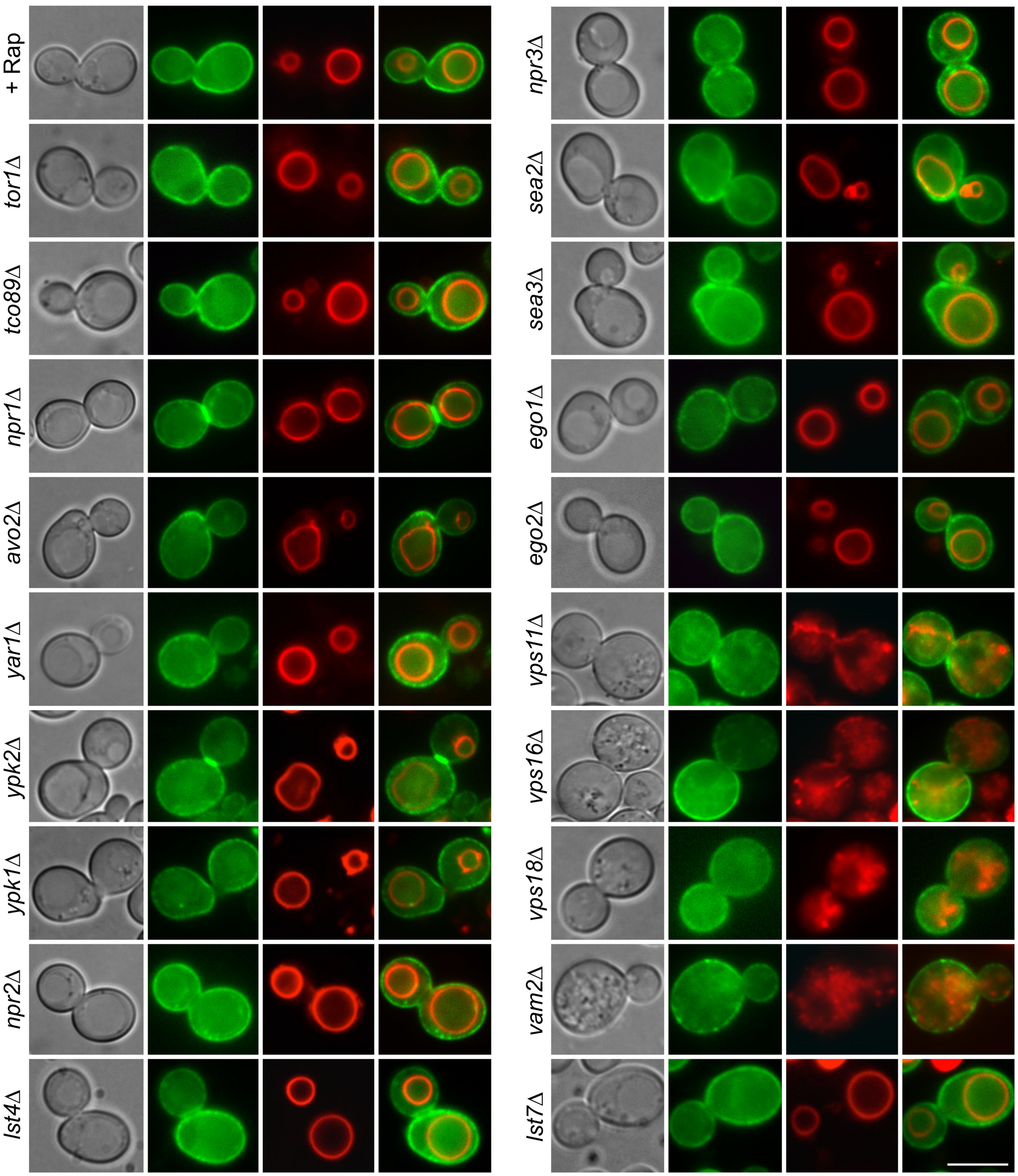
Ste3-GFP-DUb + FM4-64 (60')
Ste3-GFP-DUb + FM4-64 (60')
+ Rap
tor1Δ
tco89Δ
npr1Δ
avo2Δ
yar1Δ
ypk2Δ
ypk1Δ
npr2Δ
lst4Δ
npr3Δ
sea2Δ
sea3Δ
ego1Δ
ego2Δ
vps11Δ
vps16Δ
vps18Δ
vam2Δ
lst7Δ

B

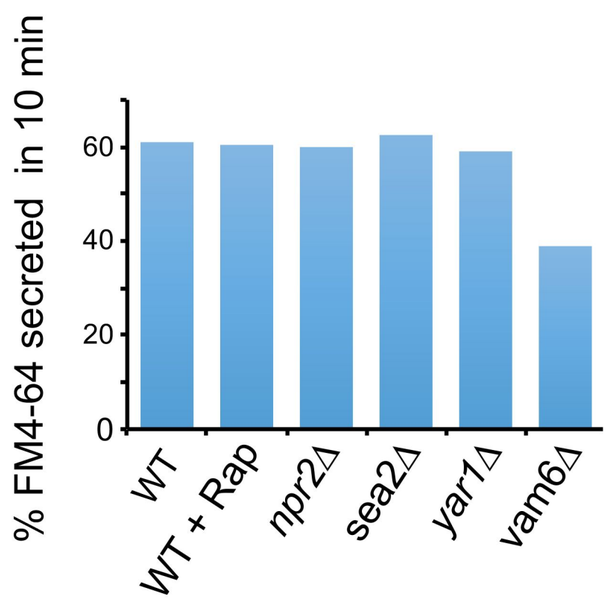
% FM4-64 secreted in 10 min
0
20
40
60
WT
WT + Rap
npr2Δ
sea2Δ
yar1Δ
vam6Δ

C

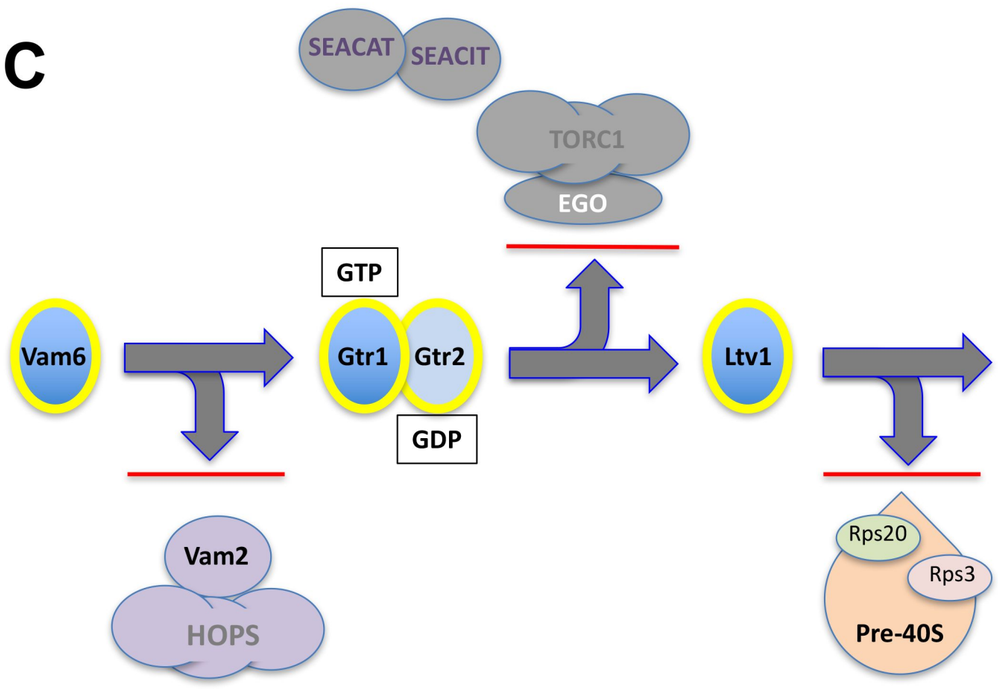
SEACAT
SEACIT
TORC1
EGO
GTP
Vam6
Gtr1
Gtr2
GDP
Ltv1
Vam2
HOPS
Rps20
Rps3
Pre-40S

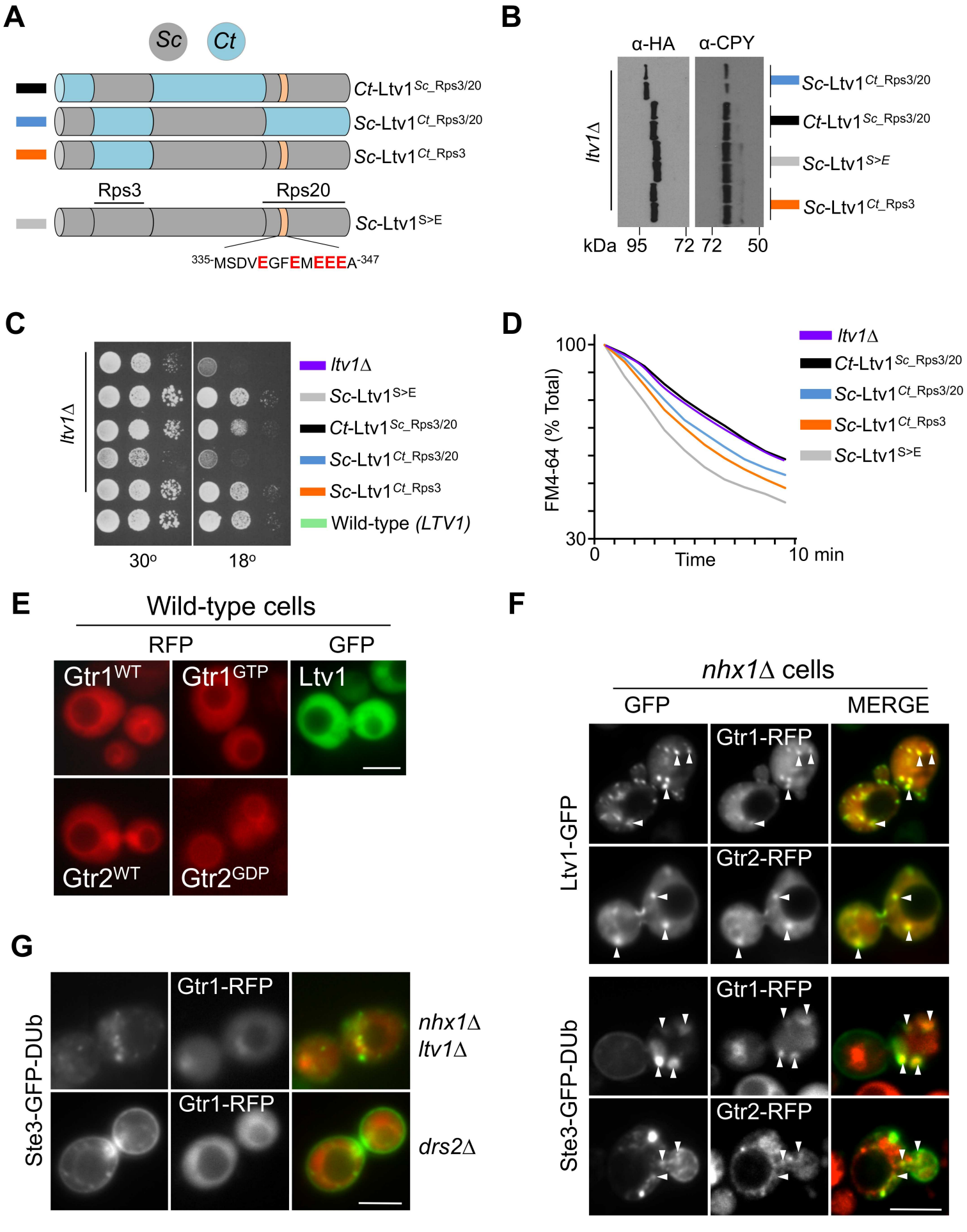
A
Sc
Ct
Ct-Ltv1 Sc_Rps3/20
Sc-Ltv1 Ct_Rps3/20
Sc-Ltv1 Ct_Rps3
Rps3
Rps20
Sc-Ltv1 S>E
335-MSDVEGFEMEEEA-347
B
α-HA
α-CPY
ltv1Δ
Sc-Ltv1 Ct_Rps3/20
Ct-Ltv1 Sc_Rps3/20
Sc-Ltv1 S>E
Sc-Ltv1 Ct_Rps3
kDa 95 72 72 50
C
ltv1Δ
ltv1Δ
Sc-Ltv1 S>E
Ct-Ltv1 Sc_Rps3/20
Sc-Ltv1 Ct_Rps3/20
Sc-Ltv1 Ct_Rps3
Wild-type (LTV1)
30º 18º
D
ltv1Δ
Ct-Ltv1 Sc_Rps3/20
Sc-Ltv1 Ct_Rps3/20
Sc-Ltv1 Ct_Rps3
Sc-Ltv1 S>E
FM4-64 (% Total)
100
30
0
Time
10 min
E
Wild-type cells
RFP
GFP
Gtr1 WT
Gtr1 GTP
Ltv1
Gtr2 WT
Gtr2 GDP
F
nhx1Δ cells
GFP
MERGE
Ltv1-GFP
Gtr1-RFP
Gtr2-RFP
Ste3-GFP-DUb
Gtr1-RFP
Gtr2-RFP
G
Ste3-GFP-DUb
Gtr1-RFP
Gtr1-RFP
nhx1Δ
ltv1Δ
drs2Δ

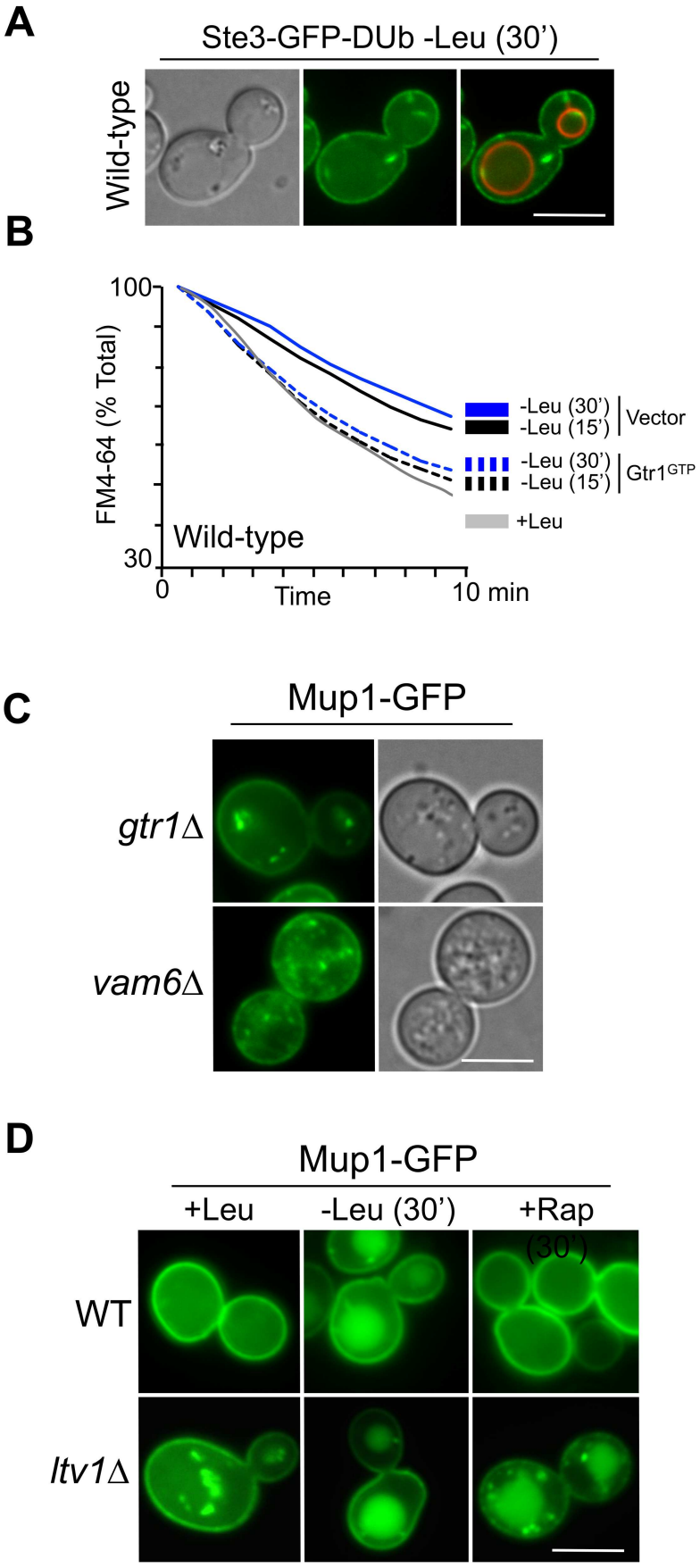
A
Ste3-GFP-DUb -Leu (30')
Wild-type
B
100
30
FM4-64 (% Total)
Wild-type
0
Time
10 min
-Leu (30')
-Leu (15')
Vector
-Leu (30')
-Leu (15')
Gtr1GTP
+Leu
C
Mup1-GFP
gtr1Δ
vam6Δ
D
Mup1-GFP
+Leu
-Leu (30')
+Rap (30')
WT
ltv1Δ